Hydrocarbon Hydroxylation by Cytochrome P450 Enzymes

Paul R. Ortiz de Montellano[*]

Department of Pharmaceutical Chemistry, University of California, 600 16th Street, San Francisco, California 94158-2517

1. Introduction to Cytochrome P450 Enzymes

In chemical terms, the regio- and stereoselective hydroxylation of hydrocarbon C-H bonds is a very difficult transformation. Nevertheless, these reactions are deftly catalyzed by a variety of metalloenzymes, among which the most diverse are the many members of the cytochrome P450 family. Cytochrome P450 enzymes are found in most classes of organisms, including bacteria, fungi, plants, insects, and mammals. Thousands of such proteins are now known (http://drnelson.utmem.edu/cytochromeP450.html), including 57 in the human genome [1], 20 in *Mycobacterium tuberculosis* [2], 272 in *Arabidopsis* [3], and the amazing number of 457 in rice [4]. The nomenclature for these enzymes is based on their sequence similarity when appropriately aligned, a somewhat arbitrary similarity cutoff (approximately >40% identity) being used to define members of a family and a higher cutoff (approximately >55% identity) members of a subfamily [5]. Thus CYP3A4 corresponds to the fourth enzyme in family 3, subfamily A. This nomenclature allows the naming of enzymes without regard to their origin or specific properties.

The mammalian, plant, and fungal proteins are commonly membrane bound and are relatively difficult to manipulate, but the bacterial proteins are usually soluble, monomeric proteins. For that reason, much of the early research on mechanisms of cytochrome P450 enzymes was carried out with bacterial enzymes, particularly with the prototypical enzyme CYP101 (P450$_{cam}$) from *Pseudomonas putida* [6,7]. From a chemist's point of view, there is a particular interest in the thermophilic enzymes, which currently include CYP119 [8-10], P450st [11], CYP174A1 [12], and CYP231A2 [13]. The thermal stability of these enzymes makes them attractive starting points for the development of industrially useful catalysts. In this context, particular attention has also focused on CYP102 (P450BM3), a self-sufficient enzyme from *Bacillus megaterium* in which the flavoprotein protein required for transfer of electrons from NADPH is fused to the hemoprotein [14]. The resulting simplicity and high catalytic rate have led to extensive efforts to engineer this protein for practical catalytic purposes [15-19]. Although these proteins have properties that make them particularly attractive for engineering purposes, the large reservoir of P450 enzymes that collectively catalyze an astounding diversity of reactions suggests that P450 catalysis will develop into a highly useful technology.

The cytochrome P450 enzymes are defined by the presence in the proteins of a heme (iron protoporphyrin IX) prosthetic group coordinated on the proximal side by a thiolate ion [20, 21]. This feature gives rise to the spectroscopic signature that defines these enzymes, as the thiolate-ligated ferrous-CO complex is characterized by a Soret absorption maximum at ~450 nm [21]. A thiolate-coordinated heme group is present in all P450 enzymes, although not all proteins with such coordination are members of this superfamily. One obvious exception, for

Address editorial correspondence to: Paul R. Ortiz de Montellano, University of California, 600 16th Street, San Francisco, CA 94158-2517, TEL: (415) 476-2903, FAX: (415) 502-4728, ortiz@cgl.ucsf.edu.

example, is chloroperoxidase, which has a thiolate-coordinated heme group but normally catalyzes a very different reaction than the P450 enzymes (21-23).

Although there are unusual P450 enzymes, such as the thromboxane and prostacyclin synthases (24), or CYP152 from *Sphingomonas paucimobilis* or *Bacillus subtilis* (25,26), that normally utilize peroxides as substrates, the defining reaction for P450 enzymes is the reductive activation of molecular oxygen. In this reaction, one of the oxygen atoms of molecular oxygen is inserted into the substrate and the other oxygen atom is reduced to a molecule of water. With one exception to date (27,28), the electrons required for this reduction of molecular oxygen derive from reduced pyridine nucleotides (NADH or NADPH). The overall equation for the reaction thus adheres to the formula: $RH + NAD(P)H + O_2 + H^+ \rightarrow ROH + NAD(P)^+ + H_2O$, where RH stands for a substrate with a hydroxylatable site. P450 enzymes therefore belong to the monooxygenase class of enzymes that only insert one of the oxygen atoms of molecular oxygen into their substrates. However, under appropriate circumstances or with specific substrates, other P450-catalyzed reactions can be observed, including desaturation, carbon-carbon bond scission, and carbon-carbon bond formation (29,30). This review specifically focuses on P450-catalyzed hydrocarbon hydroxylation, the reaction that is most characteristic of P450 enzymes and that has been most extensively investigated. However, the principles that apply in these reactions also apply to other hydroxylation reactions, including those that occur on carbons adjacent to nitrogen, sulfur, or oxygen.

2. Formation of the Catalytic Species

2.1. Overall Catalytic Cycle

The overall catalytic cycle of P450 enzymes is summarized in Figure 1. The resting enzyme is in the ferric state and has a thiolate proximal ligand. The distal ligand is usually a water molecule (**A**) (20), although a few P450 proteins do not have a ligand coordinated to the iron on the distal side (e.g., CP2D6) (31). Substrate (RH) binding results in displacement of the water ligand, if it is present, and this causes a shift in the redox potential of the heme iron atom by up to 300 mV that enables electron transfer from a redox partner to occur (**B**). The resulting ferrous, substrate-bound protein (**C**) then binds oxygen to yield the ferrous dioxy complex, which can also be represented as a ferric superoxide complex (**D**, as shown). A second electron transfer generates the ferric peroxy anion, which is protonated to give the ferric hydroperoxo complex (**E**). This second electron transfer is usually, but not invariably (32), the rate-limiting step of the catalytic cycle. The ferric hydroperoxo intermediate is unstable and, upon protonation, fragments to give a ferryl intermediate that can be formulated, as shown, as a porphyrin radical cation Fe(IV) species (**F**). Alternative formulations, shown below in Figure 1, are as a protein radical cation Fe(IV) species (**F′**) or as an Fe(V) species (**F″**). This ferryl intermediate, also known as Compound I, is two oxidation states above the resting ferric state. It reacts with the substrate to produce the hydroxylated metabolite (**G**) and, after product release and reequilibration with water, the resting ferric state of the enzyme. The key states in this catalytic cycle are individually addressed below.

2.2. Ferrous-Dioxygen Intermediate

The cytochrome P450 catalytic cycle is initiated by reduction of the heme iron atom to the ferrous state. The electrons for this reduction, depending on the specific cytochrome P450, are provided by either (a) cytochrome P450 reductase (CPR), a membrane-bound protein with an FAD and an FMN as prosthetic groups (e.g., CYP3A4, CYP2C9) (33-35), (b) an iron-sulfur protein that shuttles electrons from a flavoprotein with a single FMN prosthetic group (e.g., CYP101, CYP11A1) (33,34), or (c) a P450 reductase-like domain fused to the P450 heme domain within a single polypeptide (CYP102) (33,34,36). Isolated examples of other electron donor partners, including a flavodoxin (37), a 2-oxoacid ferredoxin oxidoreductase (28), and

a fusion protein incorporating both a ferredoxin and ferredoxin reductase into a single polypeptide with the P450 enzyme (38), have been reported. It is likely that other variants will be found, but they are likely to be of limited generality. In each instance, the function of the electron donor partner(s) is to uncouple the two electrons provided by the initial source, usually NADPH or NADH, and to transfer them singly to the P450 enzyme. The structure of ferrous P450$_{cam}$ (CYP101) has been determined (39), and it is possible that some of the structures thought to be of the ferric enzyme are actually of the ferrous enzyme, as the heme iron atom can be reduced by the x-ray beam (40).

Reduction to the ferrous enzyme is followed by binding of molecular oxygen to give the ferrous dioxy complex. This complex has been observed and characterized for P450$_{cam}$ (and occasionally for other P450 enzymes) by diverse physical techniques, including stopped flow and low-temperature spectroscopy (41-44), x-ray crystallography (39,45), Mössbauer spectroscopy (46), MCD (47), EXAFS (48), resonance Raman (49,50), and computational methods (51-53). The P450$_{cam}$ ferrous dioxy complex, with a Soret maximum at 418 nm, a β-band at 555 nm, and a very weak α-band at 580 nm, undergoes a relatively slow autoxidation ($k = 10^{-4}$ s^{-1} at pH 7.4, 4 °C) with loss of superoxide to regenerate the ferric heme (41). The Mössbauer data indicates that the complex corresponds more closely to a ferric-superoxide complex than a ferrous-dioxygen complex (46). In the crystal structure, the oxygen is bound to the iron end-on with the distal oxygen pointing towards Thr252, a distance of ~1.8 Å separating the iron from the first oxygen (39,45). Resonance Raman suggests that the Fe-O-O bond is sterically strained, perhaps facilitating its eventual rupture (50). Computational analysis of a model ferrous dioxygen complex predicts a diamagnetic singlet ground state and a predicted UV-visible spectrum consistent with that obtained experimentally (51).

2.3. Ferric Hydroperoxide Intermediate

Until recently, the ferrous dioxygen complex was the last observable intermediate in the P450 catalytic cycle. However, the ability to inject an electron into this complex by irradiation of frozen solutions of the protein at 77 K has made the ferric peroxy anion and ferric hydroperoxo complexes observable by spectroscopic and EPR methods (54-59). The electron required for this process has been introduced by radiation from a ^{60}Co gamma source, ^{32}P-enriched phosphate in the medium, or x-rays. These studies led to identification of a new species by EPR for camphor-bound P450$_{cam}$ with g-factors of 2.27, 2.17, and 1.95 that decays away when the sample is annealed at 190 K (55,56). Based on the EPR spectral properties, this spectrum was attributed to a ferric hydroperoxo intermediate with the hydroperoxy anion bound end-on to the iron rather than in a side-on arrangement with bonds from both of the oxygens to the iron. Specifically, the EPR spectrum exhibited the hallmark of a low spin ferric heme complex with $g_1 > g_2 > g_e > g_3$, not the properties of a ferrous superoxy complex in which the unpaired electron resides on the oxygens or that expected for side-on binding of the peroxo moiety with bonds from the iron to both oxygens. This conclusion is reinforced by resonance Raman analysis of the ferric hydroperoxo species (57). It is assumed that the initial reduction product is the ferric peroxo anion by analogy with analogous experiments with heme oxygenase-1, in which the ferric peroxy anion can be observed and shown to be protonated to form the ferric hydroperoxide even at extremely low temperatures by a tunneling mechanism (58). In accord with this inference, mutations of Gly248 in the distal site to a Thr or Val, mutations that dehydrate the active site and impair catalysis, also perturb the proton delivery required to generate the ferric hydroperoxide intermediate (59). Warming up the cryogenically generated ferric hydroperoxide species, also known as Compound 0, results in formation of the hydroxylated camphor product. Furthermore, if a mutant (T252A) is made that impairs proton delivery and leads to uncoupling of the enzyme rather than product hydroxylation, the intermediate is still observed but does not lead to the hydroxylated product on warming. Further studies confirmed that the initial product was the end-on hydrogen-bonded ferric peroxy anion,

which even at cryogenic temperatures was transformed into the ferric hydroperoxo intermediate (60). Reduction of the P450$_{cam}$ ferrous dioxygen complex by ^{32}P-radiation gave results entirely consistent with those obtained with a ^{60}Co source (61), as did reduction of the analogous complex of CYP119 (62).

Warming the cryogenically generated ferric hydroperoxide of P450cam resulted in formation of the normal 5-exo-hydroxycamphor in which the hydroxyl oxygen, according to ENDOR studies in normal and deuterated buffers, is coordinated to the heme iron atom (60). No evidence was obtained for accumulation of the ferryl species expected from O-O bond heterolysis. However, the finding that the oxygen of the hydroxylated product is coordinated to the heme iron atom rather than a water molecule is consistent with hydroxylation by the ferryl, as displacement of the water iron ligand expected if the ferric hydroperoxide itself was the hydroxylating agent by the product hydroxyl group would not be expected to occur at cryogenic temperatures. Comparison of the properties of the P450cam ferric hydroperoxo species generated in the presence and absence of camphor, or of 5-methylenyl-camphor, 5,5-difluorocamphor, norcamphor, or adamantanone as surrogate ligands, indicated that all of the substrates increased the lifetime of the ferric hydroperoxo intermediate at least 20-fold (63). It is notable that the T252A mutation, which suppressed the hydroxylation of camphor, did not prevent oxidation of the double bond of 5-methylenyl-camphor.

2.4. Ferryl Intermediate

2.4.1. From Molecular Oxygen—As already mentioned, efforts to detect the putative ferryl oxidizing species by cryogenic radiolysis of the ferrous dioxygen complex of P450$_{cam}$ resulted in identification of the ferryl hydroperoxide complex (Compound 0) but no other species subsequent to it before the complex of the 5-*exo*-hydroxycamphor product with the iron atom of the enzyme. The exception to this is the reported observation of the ferryl species by cryogenic x-ray crystallography (39). *In situ* reduction by the x-ray beam was shown to reduce ferric P450$_{cam}$ to the ferrous state that reacted with oxygen to give the ferrous dioxygen complex, both of which gave clear diffraction data, but further reduction of this intermediate by the x-ray beam did not yield the ferric hydroperoxide intermediate observed in other radiolytic studies. Instead, an intermediate was observed with what appeared to be a single oxygen atom bound to the heme iron atom, although the electron density map suggested only partial conversion to the observed species. The assignment of this intermediate to the ferryl species was supported by an iron-oxygen distance of ~1.65 Å, somewhat shorter than the usual iron-oxygen single bond distance of 1.8 Å. The authors stated some possible reservations concerning the assignment: for example, one electron reduction of the ferryl species should be more facile than reduction of the ferrous dioxygen species, so the ferryl should not accumulate. In view of the quality of the data for the "ferryl species", which could be due to the presence of a mixture of species that includes the hydroxylated product, and the caveats concerning its formation, interpretation of the electron density as that of the ferryl species must be viewed with some skepticism. No other radiolytic method has yielded evidence for the ferryl intermediate, as the only species observed are the ferric hydroperoxide and the product complex.

2.4.2. Peroxides as Activated Oxygen Donors—Numerous studies have been carried out of the reactions of P450 enzymes with hydrogen peroxide, alkyl peroxides, and acyl peroxides in efforts to generate a ferryl species analogous to that of Compound I of the peroxidases. EPR studies provided evidence in 1993 for the formation of a ferric alkylperoxo complex (Fe^{III}-OOR) in the reaction of a purified rat liver cytochrome P450 enzyme with *tert*-butylhydroperoxide (64). The ferric low-spin complex exhibited EPR signals at $g_1 = 2.29$, $g_2 = 2.24$, and $g_3 = 1.06$, which agree well with those of model thiolate-iron(III)-peroxo heme

complexes. This complex presumably corresponds to the already mentioned ferric hydroperoxo species obtained by radiolytic reduction of the ferrous dioxygen complex (55-57).

The reaction of P450 enzymes with alkylperoxides has been known for some time to yield a UV-visible spectrum reminiscent of a Compound II-like ferryl (Fe^{IV}=O) species in which the heme is only one oxidation equivalent higher than the resting ferric state. Early work found little evidence for formation of a Compound I-like ferryl porphyrin radical cation that is two oxidation equivalents above the resting state (65-74). However, recent work has confirmed the formation of the Compound II-like intermediate but has also identified a Compound I-like species as a transient intermediate.

The first evidence for a Compound I-like intermediate was provided by Egawa *et al.* in 1994 in studies of the reaction of *meta*-chloroperbenzoic acid (*m*CPBA) with ferric low-spin P450$_{cam}$ (73). They observed several species by rapid scan spectroscopy, the first of which had maxima at 367 and 694 nm almost identical to the absorption bands at 367 and 688 nm of Compound I of chloroperoxidase. This species appeared after 10 ms, and by 1 sec the heme was almost completely destroyed. Kellner *et al.* later used stopped flow spectroscopy to investigate the reaction of *m*CPBA with the thermostable CYP119 (75). Rapid mixing of *m*CPBA with ferric CYP119 produced several species, including an intermediate with maxima at 370, 610, and 690 nm attributed to the Compound I of CYP119. These spectral properties had to be extracted from the data by deconvolution, as only a very minor fraction of the protein (~3%) actually accumulated in the Compound I state. The rate constant for formation of this intermediate at pH 7.0 and 4 °C was estimated to be 3.20×10^5 M^{-1}s^{-1}, although the rate decreased with decreasing pH. The Compound I intermediate was reported to decay back to the ferric enzyme with a first order rate constant of 29.4 s^{-1}. Spolitak *et al.* revisited the reaction of P450$_{cam}$ with *m*CPBA in 2005 (74). They confirmed that a Compound I like species was formed to some extent at or above pH 7.0 with *m*CPBA, whereas at lower pH the only species observed had a Soret band at 406 nm that was attributed to a Compound II-like intermediate with a ferryl neutral porphyrin and, presumably, a protein radical (see below). To minimize destruction of the heme in these studies they included peroxidase substrates such as guaiacol and ascorbic acid. In further studies, Spolitak *et al.* examined the effect of Y75F and Y96F mutations on the formation of Compounds I and II (76). These mutations favored formation of Compound II, which could not hydroxylate camphor but could be reduced to the ferric state by ascorbate and other peroxidase substrates.

EPR studies indicate that the Compound II-like UV-visible spectrum is accompanied, at least to some extent, by the formation of a protein radical (70,71,74). Schünemann *et al.* investigating the reaction of P450$_{cam}$ with peracetic acid, were unable to detect a Compound I species within 8 ms (70). Using freeze-quench EPR they observed a radical with g_x = 2.0078-2.0064, g_y = 2.0043, and g_z = 2.0022, values and assigned the signal to a tyrosine radical in a polar environment. Mössbauer spectroscopy of the freeze-quenched samples confirmed that the iron was in the Fe(IV) state (68,69). Based on modeling studies they attributed the radical to the active site tyrosine residue Tyr96. This protein radical could in principle be formed by (a) rapid reduction of a Compound I-like intermediate by electron transfer from the protein, or (b) homolytic scission of the peroxide O-O bond to give an alkoxy (or hydroxyl) radical that, in turn, removes an electron from the protein. The demonstration that Compound I is formed and decays to a Compound II-like intermediate indicates that this sequence accounts, at least in part, for formation of the protein radical associated with Compound II (71,74).

2.4.3. Iodoso Compounds—Iodosobenzene (PhI=O) was introduced as a source of activated oxygen for cytochrome P450-catalyzed oxidations in 1979 (77). The use of iodosobenzene developed out of earlier studies in which NaIO$_4$ and NaClO$_2$ were employed as oxygen donors in the oxidation of steroids and fatty acids by P450 enzymes (78-81). In the

case of iodosobenzene, which is a single oxygen donor, a peroxo-iron species such as Fe-OOH cannot be involved as the oxidizing agent. Based on the reactions of model metalloporphyrins with iodosobenzene, it is believed that the oxidations supported by iodosobenzene proceed via a ferryl intermediate in which the oxygen from the reagent is transferred by the enzyme to the substrate. The finding that oxygen from labeled water was incorporated into the substrate in reactions supported by PhIO would appear to contradict this inference (82-84), but subsequent work has shown that the oxygen of PhIO exchanges with the medium in the presence of, for example, liver microsomes (83,85). The extent to which the iodosobenzene-supported reaction is a faithful model for the normal oxygen-dependent reaction has been questioned, based on a comparison of the oxidation of N-cyclopropyl-N-alkyl-*p*-chloroaniline by CYP2B1 and horseradish peroxidase (86). The iodosobenzene-supported reaction produced almost exclusively the metabolites without the cyclopropyl group, whereas the oxygen-dependent turnover of CYP2B1 generated both the N-dealkylated and N-decyclopropylated metabolites (Figure 2). The PhIO-supported CYP2B1 reaction, which resembled that catalyzed by horseradish peroxidase and H_2O_2, was attributed to a single-electron transfer mechanism that differs from that of the normal oxygen-dependent reaction. The authors concluded that the phenyliodoso-supported reaction may not be a valid mimic of the normal oxidation process. It is likely that the phenyliodoso reaction produces a Compound I species analogous to that of the normal turnover, but in the absence of a substrate, as the active site is initially occupied by the oxygen donor molecule itself. Studies with the peroxide-generated Compound I have shown that it is rapidly reduced to Compound II and a protein radical when no substrate is present (previous section). The analogy with the horseradish peroxidase reaction therefore may reflect oxidation of the amine by the Compound II, which can only act as a peroxidase but not as a normal oxygen-transfer agent. The iodosobenzene-supported reaction may be a true, if inefficient, mimic of the normal P450 oxidation in situations where Compound II would be inactive, such as the hydroxylation of hydrocarbons. It is relevant to note that iodosobenzene can itself oxidize hydrocarbon bonds, but the reaction is much slower than that observed with a model iron(IV)-oxo species (87).

2.4.4. Photolytic Ejection of One Electron from "Compound II"—Laser flash photolysis with 355 nm light of the Compound II of model iron porphyrins, horseradish peroxidase, or equine myoglobin has been reported to generate the corresponding ferryl porphyrin radical cations characteristic of Compound I (88). In these studies Compound II was generated by reaction of the ferric precursor with either PhIO or H_2O_2. As Compound I is generated essentially instantly, this approach makes possible kinetic studies at very short time scales.

In a subsequent study the photolytic approach, applied to an iron corrole Compound II, yielded a transient species that decayed rapidly. This species was tentatively attributed to a corrole Fe(V)=O rather than an Fe(IV)=O corrole radical cation based on its UV-vis spectrum, reactivity, and analogy with previous studies of model manganese porphyrins (89). Inclusion of *cis*-cyclooctene and ethylbenzene in this photolysis reaction resulted in the formation of *cis*-cyclooctene oxide and 1-phenylethanol (89). Estimates of the rates of oxidation of these substrates based on the increased rate of disappearance of the reactive intermediate as a function of substrate concentration gave rates of 5900 M^{-1} s^{-1} for cyclooctene and 570 $M^{-1}s^{-1}$ for ethylbenzene oxidation.

In a further model study, laser flash photolysis was investigated with 5,10,15,20-tetramesitylporphyrinatoiron(III) as the model system (90). Again, photolysis of the Compound II equivalent yielded a transient oxidizing species that reacted 5-orders of magnitude faster with substrates such as diphenylmethane, ethylbenzene, *cis*- and *trans*-stilbene, and cyclohexene than the known Compound I analogue Fe(IV)=O porphyrin radical cation. An alternative reagent for formation of the hypervalent oxidizing species has been

reported in which iron porphyrins were first converted to transient iron(IV) diperchlorates, and then by photolysis to a new oxidizing species postulated to be the Fe(V) porphyrin (91). The reactive species thus obtained oxidized styrene, stilbene, cyclohexene, ethylbenzene and other substrates at rates 4-5 orders of magnitude faster than the corresponding Por+·Fe(IV)=O electronic isomers.

One anomaly relevant to enzymatic reactions is the fact that in none of the model reactions was a proximal thiolate ligand required for the high oxidation rates. That is, the model studies apply equally well to the reactive species formed by, for example, classical peroxidases as to cytochrome P450 enzymes. However, peroxidases, even if mutated to allow better substrate access to the heme center, are very poor catalysts of reactions such as hydrocarbon hydroxylation. In principle, the model studies should actually be better mimics of peroxidase than P450 enzymes due to the proximal ligands involved in the models, yet the reactivity seen with the models is not observed with the peroxidases. This suggests that the highly reactive species obtained in the irradiation reaction, whatever its detailed nature, may not be related to the oxidizing species in enzymatic reactions. It should be noted, in this context, that calculations suggest that the PorFe(V)=O species is sufficiently higher in energy than the more conventional Por+·Fe(IV)=O species to be a viable oxidizing species in enzyme catalysis (92,93).

In the first application of this approach to a P450 enzyme, Compound II of CYP119 was first generated by reaction of the ferric enzyme with peroxynitrite, a reaction that resulted in a species with a Soret band at 429 nm rather than the starting 416 nm (94). The resulting spectrum was similar to that of the known Compound II of chloroperoxidase, another heme thiolate protein. Laser irradiation at 355 nm converted approximately 5% of this Compound II to a new species with a broad Soret absorption in the 400-410 nm region. This intermediate was assigned to a Compound I species that appeared surprisingly stable, decaying at 20 °C with a lifetime of ~200 ms. This decay time did not change appreciably in the presence of lauric acid, a known substrates of the enzyme. Based on this apparent low reactivity, it was suggested that the actual oxidizing species in cytochrome P450 catalysis might be an Fe(V)=O precursor of the conventional Compound I intermediate.

Formation of the starting Compound II by reaction of ferric P450 with peroxynitrite was subsequently challenged by a report that the reaction of P450BM3 with peroxynitrite gives rise to an Fe(III)-NO complex rather than to Compound II (95). However, it appears that the reaction can give both Compound II and the Fe(III)-NO complex, the former being short lived and the latter a stable product (96). The results confirm that the species utilized in the photolysis work was, indeed, Compound II. One aspect neglected early in this debate is the fact that peroxynitrite reacts not only with the iron but also with the protein. Peroxynitrite has been shown to promote the nitrosylation of tyrosines and other reactions (97), and protein modifications of this type could conceivably alter the kinetic values for decay of the reactive intermediate and/or substrate oxidation. However, it has recently been reported that reaction of CYP2B4 with peroxynitrite results in incorporation of approximately three nitro groups, but these modifications did not significantly alter the catalytic activity (98). Thus, at least in this instance, nitration was not a confounding factor.

More recently, Newcomb has used the peroxynitrite-CYP119 system to generate Compound I and used it to carry out kinetic studies of its ability to oxidize hydrocarbon and olefin substrates (99). The UV-vis spectrum of the Compound I intermediate was somewhat better defined in this study and shown to have Soret maxima at ~367 and ~416 nm, and a Q-band at ~650 nm, properties that suggest it is a conventional Por+·Fe(IV)=O species. ^{18}O studies established that the oxygen incorporated into the substrates derived from peroxynitrite, as predicted by the photolysis approach. The rates (k_{app}) for the oxidation by Compound I were benzyl alcohol, (2.7×10^4 $M^{-1}s^{-1}$), ethylbenzene (2.5×10^3 $M^{-1}s^{-1}$), lauric acid (7.2×10^2 $M^{-1}s^{-1}$), methyl

laurate (1.2×10^3 M^{-1}s^{-1}), styrene (7.6×10^3 M^{-1}s^{-1}), and 10-undecenoic acid (9.5×10^3 M^{-1}s^{-1}). Interestingly, lauric acid, the only one of these that is a known substrate under normal catalytic turnover conditions, is the slowest oxidized. This suggests that the limited substrate specificity of CYP119 is largely determined by a requirement for substrate interactions for the formation of Compound I via the normal electron transfer pathway that is more restrictive than the limitations imposed on oxidation of substrates once it is formed. Although the CYP119 Compound I species is less reactive than that of P450$_{cam}$, the results of these studies did not require postulation of a species other than the conventional Compound I as the hydroxylating intermediate.

In an extension of the work with CYP119, the peroxynitrite and photolysis approach has been utilized to examine the oxidation of benzphetamine by cytochrome P450 2B4 and mutants of this protein (98). The peroxynitrite-photolysis sequence was found to give a spectrum consistent with that of Compound I of chloroperoxidase and this intermediate was shown to oxidize benzphetamine, a conventional substrate of the enzyme. Comparison of the rates of this oxidation by CYP2B4 and CYP119 led to two conclusions: (a) that the reactive oxidizing species had similar reactivities in the two enzymes, and (b) that the efficiency of substrate oxidation was strongly controlled by the binding affinity of the enzyme for the substrate. There was no evidence in these studies for the accumulation of a Compound I species other than that represented by the Por+·Fe(IV)=O intermediate.

3. Oxygen Insertion into the C-H Bond

3.1. Mechanism

The mechanism of hydrocarbon hydroxylation cannot be divorced from the question of the nature of the oxidizing species generated in cytochrome P450 catalysis. In the sections below, we will first consider the most widely accepted hydroxylation mechanism, which assumes that the hydroxylating species is a Por+·Fe(IV)=O species. Alternative hydroxylation mechanisms will be considered with respect to this first mechanism, generally known as the radical rebound mechanism.

3.1.1. Retention of Stereochemistry—A substantial body of data indicates that the hydroxylation of hydrocarbon C-H bonds usually proceeds with retention of configuration at the reacting carbon. In early publications it was reported that the P450-catalyzed 7α-hydroxylation of cholesterol and 11α-hydroxylation of pregnane-3,20-dione proceed with retention of stereochemistry (100,101). Even more impressive is the finding that acyclic compounds, which are less sterically constrained in their motion, can also be hydroxylated with retention of stereochemistry. Thus, incubation of (1R)- and (1S)-[1-^{3}H,^{2}H,^{1}H:1-^{14}C] octane with rat liver microsomes gave mixtures of 1-octanol products in which the hydroxyl was introduced without loss of the carbon atom stereochemistry (Figure 3A) (102). In a related elegant example, the oxidation of (R)-(8-^{2}H$_1$)[8-^{3}H$_1$]- and (S)-(8-^{2}H$_1$)[8-^{3}H$_1$]geraniol by a microsomal P450 enzyme from *Catharanthus roseus* was shown by NMR analysis to proceed with complete retention of both regiochemistry and stereochemistry (Figure 3B) (103). These studies illustrate the general rule that hydroxylations catalyzed by cytochrome P450 usually proceed with retention of stereochemistry. However, it is the abnormalities in a reaction that usually provide the most revealing mechanistic information.

3.1.2. Radical Rebound—The radical rebound mechanism in the context of cytochrome P450 was first proposed in 1978 in a short communication by Groves, McClusky, White, and Coon (104). The mechanism proposed by these authors was formulated to explain the finding that (a) the hydroxylation of norbornane by a liver microsome preparation gave *exo*- and *endo*-2-norborneol in a 3.4:1 ratio, (b) oxidation of 2,3,5,6-tetradeuteronorbornane gave the same products in a 0.76:1 ratio, and finally, (c) that 25% of the exo-norborneol retained four

deuterium atoms while 9% of the *endo*-norborneol only retained three deuterium atoms. Thus, the hydroxylation proceeded with a large degree of inversion of stereochemistry at the carbon undergoing hydroxylation and was subject to a large ($k_H/k_D = 11.5$) primary isotope effect (Figure 4). The hydrogen abstraction followed by rebound hydroxylation mechanism proposed to explain these results was based on involvement of an Fe(V)=O species as the hydroxylating agent (as shown), but works equally well for a Por+·Fe(IV)=O oxygenating intermediate. In this mechanism, the ferryl oxygen abstracts a hydrogen from the substrate, leaving a carbon radical on the substrate, which in turn recombines with the equivalent of a hydroxyl radical coordinated to the iron atom. This mechanism would be subject to a large intramolecular isotope effect if C-H bond breaking is rate limiting after formation of the reactive species, and loss of stereochemistry could occur after hydrogen abstraction and prior to recombination of the carbon radical with the hydroxyl radical equivalent. The ratio of the *exo-* and *endo*-hydroxyl products from a given radical intermediate would then depend on the rate of the hydroxyl rebound relative to the rate of substrate repositioning within the active site.

3.1.2.1. Isotope Effects: The key findings of this first study, a large intramolecular isotope effect and, in some instances, partial loss of either stereo- or regiochemistry in the hydroxylation reaction, have been confirmed by numerous studies. Thus, a large intramolecular isotope effect ($k_H/k_D = 11$) was observed during hydroxylation of 1,3-diphenylpropane in which one pair of benzylic hydrogens were replaced by deuterium and the other pair remained as hydrogens (Figure 5A). Large intramolecular isotope effects, with values ranging from $k_H/k_D = 4$ to 18, depending on initial stereochemistry, were also observed in the hydroxylation of (*R*)- and (*S*)-1-^{2}H-ethylbenzene (Figure 5B) (105). An analysis by the Northrop method of the isotope effect in the 6β-hydroxylation of 6β-deuterated and tritiated testosterone by CYP3A4 found an isotope effect of 15 associated with the hydroxylation reaction (Figure 5C) (106).

Although large intrinsic isotope effects are associated with the hydroxylation of substrates that can be rapidly repositioned within the active site, isotope effects can be masked to different degrees if substrate mobility is impaired and the substrate cannot be easily repositioned within the time frame of the hydroxylation process. Thus, the benzylic hydroxylation of mono-, di-, and trideuterated xylenes by rat liver microsomes and CYP2B1 gave primary isotope effects ranging from $k_H/k_D = 5.32$ to 7.57 (107). This deuterated xylene data suggested that the 6.62 Å distance between the methyl groups of *para*-xylene is insufficient to mask the intrinsic isotope effect (Figure 6). However, analogous studies with deuterated 4,4′-dimethylbiphenyl showed that the hydroxylation isotope effect in the oxidation of this substrate, in which the methyl groups are separated by a distance of 11.05 Å, is almost completely masked. Similar results were obtained when the studies were extended to CYP2E1 and CYP2A6: the (k_H/k_D)$_{obs}$ values for CYP2E1 were 9.03 for *o*-xylene, 6.65 for *m*-xylene, 6.04 for *p*-xylene, and 2.28 for 4,4′-dimethylbiphenyl; for CYP2A6 the corresponding values were 11.46, 7.21, 5.53, and 1.07 (108). A follow up experiment with CYP101, for which a crystal structure is available, gave observed isotope effects for the substrates with one trideuterated methyl group of 10.6 for *o*-xylene, 7.4 for *p*-xylene, and 2.7 for 4,4′-dimethylbiphenyl (109). Molecular dynamics simulations were carried out with the compounds bound in the CYP101 active site and the mobility of the substrates was shown to decrease in the order *o*-xylene > *p*-xylene > 4,4′-dimethylbiphenyl, in accord with the conclusion that decreased mobility and increased distance between the competing groups masked the isotope effect.

Strong evidence indicates that more than one substrate molecule can be bound in the active site of some P450 enzymes. Analysis of the isotope effects in the CYP2A6-catalyzed hydroxylation of the xylene isomers with one deuterated methyl group shows that binding of a second molecule in the active site increases masking of the isotope effect, as would be expected if the steric bulk of the second molecule decreases the mobility of the xylene and thus increases masking of the isotope effect (110). Thus, the isotope effect for CYP2A6-catalyzed

oxidation of *m*-xylene with one deuterated methyl was k_H/k_D = 9.8 at 2.5 µM substrate concentration but 4.8 when the substrate concentration was increased to 1 mM.

The isotope effects in P450-catalyzed hydroxylations have generally been determined by intramolecular competition between equivalent sites, such as the two methyls in the xylenes, because direct measurements of the isotope effects on the reactions of the activated hydroxylating species were not possible. Newcomb has recently used photolytic generation of the reactive oxidizing species in CYP119 and CYP2B4 to directly measure the isotope effects for the hydroxylation of (*S,S*)-2-(*p*-trifluoromethylphenyl)cyclopropylmethane with one, two, or three deuterium atoms on the methyl group (111). The primary isotope effects obtained in these studies were k_H/k_D = 9.8 for CYP119 and 8.9 for CYP2B4.

3.1.2.2. Loss of Regio- or Stereochemistry: The inversion of stereochemistry observed in the oxidation of deuterated norbornane by liver microsomal P450 (Figure 4) is only the first example of a reaction that involves loss of regio- or stereochemistry during the hydroxylation process. In a structurally related example, the oxidation of 5-*exo*- and 5-*endo*-deuterated camphor by CYP101 (P450cam) was found to involve removal of either the 5-*endo* or 5-*exo* hydrogen but delivery of the hydroxyl group exclusively to give the *exo*-alcohol (Figure 7) (112). As these results showed, a large fraction of the reaction that occurred involved inversion of stereochemistry at the reacting carbon, a finding that implicated the involvement of an intermediate in the reaction sequence. A similar conclusion was reached when a derivative of camphor in which the carbonyl group was replaced by an *exo*-benzamido (PhCONH-) group was oxidized by a P450 enzyme from *Beauveria sulfurescens* (113). In this instance, the *exo*-alcohol was exclusively obtained and there was high retention of deuterium regardless of whether one initially had an *endo*- or *exo*-deuterium atom. The hydroxylation of 1-[²H]-ethylbenzene to 1-phenylethanol (Figure 5B) by a rabbit liver P450 enzyme has been shown to proceed with 23-40% loss of stereochemistry (105).

Loss of regiochemistry is also observed in some P450 hydroxylation reactions. Thus, an allylic transposition is observed in the hydroxylation of 3,4,5,6-tetrachlorocyclohexene by rat or housefly microsomes (Figure 8A) (114), 3,3,6,6-tetradeuterated cyclohexene (Figure 8B), methylenecyclohexane (Figure 8C), and β-pinene (Figure 8D) by CYP2B4 (115), and linoleic acid (Figure 8E) by rat liver microsomes (116). A stereospecific hydrogen abstraction from C-11 is followed by suprafacial addition of the hydroxyl to either C-9 or C-13 in the allylic transposition that converts linoleic acid to 9-hydroxyoctadeca-10*E*,12*Z*-dienoic acid or 13-hydroxyoctadeca-9*Z*,11*E*-dienoic acid. When observed, these allylic rearrangements usually occur in a minor but significant fraction (20-40%) of the hydroxylation reaction, as might be expected from recombination of an intermediate with an iron-bound hydroxylating species.

The oxidation of (*R*)-(+)-pulegone to menthofuran by rat liver microsomes results in an allylic transposition that is, unusually, also accompanied by isomerization about the double bond prior to conversion of the intermediate to an alcohol precursor, presumably by transfer of the hydroxyl radical equivalent to the substrate carbon radical (Figure 9) (117).

The oxidative cleavage of a carbon-carbon bond with release of acetone in the biosynthesis of psoralen from (+)-marmesin by enzymes of the CYP71AJ family provides independent evidence for the intervention of an intermediate in carbon hydroxylation (Figure 10) (118-120). In this reaction, hydrogen abstraction from the β-carbon of a dihydrofuran ring generates a radical (or cation) that undergoes loss of a $(CH_3)_2CH(OH)$-substituent attached to the α-carbon, resulting in the introduction of a double bond and the formation of a molecule of acetone. This reaction has been formulated as involving an initial radical intermediate, but it can also be envisaged as proceeding via a cationic intermediate. Substitution of deuterium for the hydrogens on the β-carbon results in a metabolic shift to oxidation of another position,

confirming the proposal that the reaction is initiated by hydrogen abstraction from the β-carbon (120).

3.1.2.3. Radical Clocks: The greatest effort in elucidation of the P450 mechanism through the analysis of rearrangements that accompany hydrocarbon hydroxylation has been put into studies of radical clock substrates. A radical clock denotes a compound which, when converted to a radical by hydrogen abstraction, can either immediately collapse to give an unrearranged product or can competitively undergo a rearrangement to give a second radical that gives rise to a distinct product. If the rate of the rearrangement reaction is known and if it is not altered by being constrained within an enzyme active site, it is possible to estimate the rate of the reaction that traps the initial radical from the ratio of unrearranged to rearranged products. In all the radical clock substrates utilized for studies of hydrocarbon hydroxylation by P450 enzymes, the radical rearrangement in question is that of an appropriately substituted cyclopropylmethylene radical to a homoallylic radical (Figure 11).

The first successful radical clock experiment was provided by the observation that bicyclo [2.1.0]pentane, which gives a radical that rearranges to a monocyclic radical at a rate of 2.4×10^9 s^{-1} (121,122), gives a mixture of ring opened and unrearranged hydroxylation products from which a rate $k_t = 1.4 \times 10^{10}$ s^{-1} was calculated for the "oxygen rebound "step in which the carbon radical combines with the iron-bound "hydroxyl radical"(Figure 12,Table 1) (121, 123). The *endo*-hydrogen cis to the fused cyclopropane ring was predominantly removed and the hydroxyl added almost exclusively to the same side (123) This unique stereochemistry was first attributed to positioning by the enzyme active site (123), but subsequent experimental and computational studies suggest that at least some of this specificity is inherent in the bicyclo [2.1.0]pentane system (124,125).

A series of relatively simple alkyl-substituted cyclopropanes were then evaluated as radical clocks for the P450 hydroxylation reaction (Table 1). Although cyclopropylmethane (**2**) and 1,1-dimethylcyclopropane (**3**) did not give detectable rearrangement products, presumably because their ring opening reactions did not compete sufficiently with trapping of the radical by the activated oxygen, ring opened products were obtained with *cis-* and *trans*-1,2-dimethylcyclopropane (**4, 5**), 1,1,2,2-tetramethylcyclopropane (**6**), hexamethylcyclopropane (**7**), and two fatty acids with a cyclopropane ring in the chain (**8**). All of these radical clocks gave estimated times for the radical rebound reaction of between 1.5×10^{10} and 2.6×10^{11} s^{-1}. A value of $\sim 2 \times 10^{10}$ s^{-1} was similarly obtained when the oxidation of norcarane (**9**) was examined (126). The oxidation of norcarane is complicated by the formation of multiple products, including secondary oxidation products and a product implicating a cationic intermediate (see later section). This has led one of the two groups investigating this reaction to report that they could not provide evidence for a radical rearrangement product (127,128), although such evidence was found in the other study (126). In sum, the studies with alkyl-substituted cyclopropane rings are consistent with the intervention of a radical intermediate and a rebound rate of $\sim 10^{10}$-10^{11} s^{-1}.

Somewhat different results were obtained with radical clocks that rearrange at increasingly rapid rates due to the presence of suitably positioned aromatic rings to stabilize the ring-opened radicals (Table 1). No ring-opened products were detected in the oxidation of benzylcyclopropane (**10**), but rearranged alcohol products did result from the oxidation of 2,2-diphenylcylopropylmethane (**11**), *trans*-2-phenylcyclopropylmethane (**12**), and probes **13**-**17**. However, the radical combination indicated by the ratios of rearranged to unrearranged alcohol products for these probes were in the order of 10^{12} s^{-1}. Indeed, with probe **18**, the radical combination rate obtained was 1.4×10^{13} s^{-1}! This radical combination rates, particularly the last one, approach the rate of molecular vibrations and are more consistent with a transition state than a true radical intermediate in the hydroxylation reaction.

A third class of radical clock probes has been introduced that incorporates two simultaneous clock mechanisms, only one of which has been calibrated, to monitor the formation of radical intermediates at the reacting carbon atom (Figure 13) (129, 130). Thus, the oxidation of α- and β-thujone (**19**,**20**) at the C-4 position can result in trapping of a radical intermediate to give unrearranged alcohol, ring opening of the radical prior to trapping to give the monocyclic alcohol, and finally inversion of the stereochemistry of the C-4 radical to give the alcohol with the inverted stereochemistry. Based on the rate of the ring opening reaction, it has been estimated for a variety of P450 enzymes that the radical trapping reaction has a rate between 0.7 and 12.5×10^{10} s^{-1}. This rate is very similar to that obtained with other alkyl-substituted cyclopropyl probes. The rate of the inversion of stereochemistry at C-4 cannot be numerically calibrated but is very fast, in agreement with the finding that inversion occurs in a large proportion of the hydroxylated product formed from α-thujone by some of the mammalian P450 enzymes.

3.1.2.4. Probes for Cationic Intermediates: A number of the radical clocks have the capacity to differentiate radical from cation intermediates in P450-catalyzed hydroxylation reactions. Newcomb and coworkers cleverly designed a radical clock probe not only to search for evidence of radical intermediates, but also to evaluate the extent to which the oxidation of a methyl group on a cyclopropyl ring involved a cationic intermediate (Figure 14) (131). The principle of the probe is that the radical favors opening of the cyclopropyl ring bond that places the unpaired electron next to the phenyl ring (path a), where it can best be stabilized by resonance, whereas the cation favors an opening of the cyclopropyl ring that favors stabilization of the cationic charge by the electron pair on the oxygen atom (path b). The probe does not, however, differentiate the two possible mechanisms for formation of a cation intermediate: (i) direct formation of the cation in the initial oxidation reaction (path b), or (ii) oxidation of an initial radical to the cation by electron transfer to the oxidizing species (path c). The oxidation of this probe was examined with CYP2B1, CYP2B4, and CYP2E1, as well as mutants of these enzymes without the distal threonine involved in oxygen activation (131). Based on a radical rearrangement rate (path a) of 1.6×10^{11} s^{-1}, the rate of combination of the radical intermediate with the activated oxygen was calculated to be between 5×10^{12} and 1.2×10^{13} s^{-1}, depending on the particular enzyme used in the study. These values, as noted for some of the radical clock results already discussed, are very high and appear to suggest that they report on a transition state rather than a discrete intermediate. Furthermore, the cationic product was obtained in incubations with all the enzymes examined, the extent of the cation product accounting for ~2-15% of the products derived from oxidation of the cyclopropylmethyl group.

Other probes have been used that distinguish cation-derived products, including several of the radical clock probes already described. Norcarane, as shown in Table 1, rearranges via a radical pathway to give the (2-cyclohexenyl)methanol product, but as a cation undergoes a ring expansion and yields, after trapping by a hydroxyl group, cyclohep-3-en-1-ol (Figure 15A) (126,127). Small amounts (~0.6%) of this product were obtained in the oxidation of norcarane by CYP101, CYP102, CYP2B1, and CYP2E1, indicating that a small fraction of the oxidation of this compound proceeded via a cationic intermediate. Small amounts of cationic products were also obtained in the P450-mediated oxidation of the radical clock probes α- and β-thujone (Table 1, **19** and **20**) (130). Solvolysis experiments have shown that formation of a C-4 cation result in aromatization of the ring to give carvacrol (Figure 15B), a product that accounted for a trace (0.1-0.4%) of the metabolites with CYP101 and CYP102, but 3- 4% with CYP3A4 and CYP2D6. A further example is provided by a cubane derivative (Figure 15D) (131). The cation-derived product was not observed in incubations of CYP2B1 or CYP2B4, but was found to account for up to ~30% of the methyl group oxidation product when the distal threonine residue of CYP2B4 and CYP2E1 was mutated to an alanine. The fatty acids with a cyclopropyl ring in the chain also differentiate radical and cation reactions. The radical rearrangement product is shown in Table 1, entry 8, whereas two different products are expected if a cation

intermediate is formed (Figure 15C). However, with these substrates, none of the cation products could be detected despite the observation of radical rearrangement products (132, 133).

The products of a cationic intermediate unmasked by the reactions above account for a trace of the products formed by the native P450 enzymes. Another reaction that may involve a cationic intermediate, the introduction of a double bond between two carbons, neither of which is attached to a heteroatom, is sometimes a major reaction pathway. However, the evidence for a cation provided by this desaturation process is tainted by the fact that a mechanism can be formulated that only requires a radical intermediate. This reaction was investigated in detail for the desaturation of valproic acid to 2-propyl-4-pentenoic acid (137-141). The introduction of a double bond into the valproic acid hydrocarbon terminus is readily rationalized by two mechanism (Figure 16). Both of these mechanisms are initiated by hydrogen abstraction from the ω-1 carbon of valproic acid. The resulting radical can then be oxidized by the enzyme to the cation, which is deprotonated at the terminal carbon by the iron bound hydroxyl group to give the desaturated metabolite. Alternatively, the iron-bound hydroxyl radical equivalent can abstract the terminal hydrogen, giving the same final products. If the deprotonation step occurs at the ω-3 rather than ω-carbon, the $\Delta^{3,4}$ rather than $\Delta^{4,5}$-desaturated product is formed. The mechanisms in Figure 16 are supported, but not clearly distinguished, by the following observations: (a) the 3- and 4-hydroxylated metabolites of valproic acid are formed but are not converted to the unsaturated compounds (140); (b) a primary isotope effect of $k_H/k_D = 5.05$ is observed for 4-hydroxylation of the substrate with two deuteriums on C-4, and this isotope effect is similar to that seen for $\Delta^{4,5}$-desaturation of the same substrate ($k_H/k_D = 5.58$) (141); (c) only a small isotope effect ($k_H/k_D = 1.62$) is observed in desaturation of the compound with a trideuterated terminal methyl group (141). The isotope effects for hydroxylation and desaturation of valproic acid to give the $\Delta^{3,4}$-unsaturated valproic acid are less informative due to the incidence of metabolic switching from initial C-3 hydrogen abstraction to C-4 abstraction when deuterium is placed at C-3 and vice versa (142). The ratio of hydroxylation to desaturation is enzyme dependent, but ranges from 37:1 for CYP2B1 to 2:1 for CYP4B1 (142). These results indicate a mechanism in which abstraction of the first hydrogen from C-4 is subject to a substantial isotope effect, as expected for a hydrogen abstraction, but removal of the second hydrogen to give the double bond occurs without a significant isotope effect, as might be expected for deprotonation of a C-4 cationic intermediate or abstraction of a second hydrogen from the radical intermediate.

Numerous other instances of P450-catalyzed desaturation of unactivated carbon-carbon bonds are known in which the corresponding hydroxylated product is also formed (Table 2). These include desaturation of the ethyl group in 4-ethylbenzoic acid (**21**) (143), the isopropyl group in β-thujone (**22**) (130,144), the isopropyl group of ezlopitant (**23**) (145), the 6-desaturation of testosterone (**24**) (146), the 6-desaturation of lovostatin (**25**) (147), and the 11-desaturation of lauric acid (**26**) (148). In the case of β-thujone, testosterone, and lauric acid isotope effect experiments indicate that hydrogen abstraction from the carbon that is also hydroxylated is the rate-limiting step in the dehydrogenation process. Other instances of cytochrome P450-catalyzed dehydrogenation are known in which the hydroxylated product is not formed at all, but examples of those are not included as the focus here is on the support provided by this process relative to a hydrogen abstraction mechanism for the hydroxylation and the possible incidence of a cationic intermediate.

3.1.3. Computation—Computational approaches have made major contributions over the past two decades to clarification of the mechanism of cytochrome P450 enzymes, including a proposed solution for the discrepancies in the radical clock results. As recent advances in this area are reviewed in detail in another article in this issue (93), the computational aspects of the P450 mechanism are not covered here. However, it is worth briefly touching on a solution to

the discrepancies in the radical clock suggested by the computational work. As already discussed, radical clocks in which the initial radical is on a secondary carbon generally give results consistent with a mechanism in which the radical functions as a true intermediate, whereas so-called ultrafast clocks, in which the radical is on a primary carbon, give radical recombination rates that are so fast that they are suggestive of a transition state rather than a radical intermediate. Computation suggests that hydrogen abstractions by the P450 ferryl species give two intermediates, one in a low (doublet) spin state and the other in a high (quartet) spin state. In the low spin state, the unpaired electron residing on the substrate after hydrogen atom abstraction by the ferryl species has an opposite spin to the electron in the iron-hydroxyl orbital with which it recombines to form the hydroxylated product (Figure 17). The collapse of this radical pair is barrierless and, in observational terms, essentially identical to a concerted insertion of the oxygen into the C-H bond. In the high spin state, the substrate-based radical has the same spin orientation as that of the P450 iron-hydroxyl species. A spin-inversion barrier therefore exists that must be overcome to form the hydroxylated product. The radical clock rearrangement can compete with collapse to the hydroxylated product in the high spin intermediate, but in the low spin state cannot compete with barrierless collapse to the hydroxylated product. Thus, the ratio of rearranged to unrearranged hydroxylated products, from which the rate of the hydroxyl rebound is determined, includes not only the products formed in the high spin reaction, but also the unrearranged product formed in the low spin pathway. The ratio is thus biased in favor of the unrearranged product by the extent of the low spin reaction, resulting in calculation of a faster rate of the radical rebound to give the hydroxylated product than would be obtained from the ratio produced exclusively by the high spin pathway in which the radical clock is operative.

3.2. Specificity

The specificity of substrate hydroxylation by P450 enzymes is determined by three factors: (a) the affinity of the substrate for the P450 active site, which is controlled by the substrate lipophilicity and its compatibility with the P450 active site architecture, (b) the intrinsic reactivity of the individual C-H bonds in the substrate, which is largely determined by the C-H bond strength, and (c) the constraints imposed by the active site on the oxidation reaction by orienting the substrate relative to the iron-bound oxidizing species and by restricting its mobility.

3.2.1. Lipophilicity—The congruence of the substrate structure with that of the P450 active site is case-specific and is not discussed here, but lipophilicity is a generic parameter that is applicable to all P450 oxidations. A direct correlation of lipophilicity with K_m or K_d has been repeatedly observed and has been incorporated into numerous Hansch relationships for individual series of compounds (e.g., 149-151). For example, White and McCarthy showed that the catalytic turnover of a range of *para*-substituted toluene derivatives by a rabbit P450 enzyme was effectively described by the Hansch equation: $\log k_{cat} = 0.40\pi - 0.64\sigma + 0.79$ (149). The π-term in this equation corresponds to the lipophilicity. The link between the lipophilicity and binding to the enzyme is more explicit in one of many correlations noted by the Hansch group, in this case a correlation of the K_s (K_d determined spectroscopically) for the binding of a series of pyrazoles to microsomal cytochrome P450: $\log 1/K_s = 1.01 \log P + 2.93$ (150,152). Similarly, a nice correlation has been reported between the $-\log K_m$ values for the turnover of a series of substrates by CYP2B6 and their octanol-water log P values (151). The correlation between lipophilicity of the substrate and binding to P450, given that the substrate is compatible with the P450 active site, is not surprising, as the active sites of P450 enzymes are encased by the protein structure and are universally lipophilic.

3.2.2. Bond Strength Correlation—The first clear demonstration of the relative intrinsic reactivity of C-H bonds towards hydroxylation by cytochrome P450 was provided by early

studies on the site of oxidation of heptanes by microsomal P450 (153). Quantitation of the products from oxidation of the various isomers indicated that the oxidation had occurred with a preference for the following order of C-H bond oxidation: tertiary > secondary > primary (Figure 18). In the schematic representation in this figure, two equivalent positions are shown with half of the total alcohol metabolite generated at those sites. In every instance, the tertiary carbon, if present, is the favored site of oxidation even if there are more secondary or primary sites. This is best illustrated by the oxidation of 2-methylpropane, which has nine primary C-H bonds but only one tertiary bond, yet undergoes oxidation almost exclusively at the tertiary C-H bond. The same relationship is observed for secondary C-H bond oxidation in preference to primary C-H bonds, as is readily seen in the product distribution from *n*-heptane. These small substrates were chosen, in part, to minimize the control of the oxidation by the P450 active site structure, thus allowing the intrinsic selectivities to be observed. Clearly, steric accessibility to the C-H bonds is not the critical parameter, although steric effects do enter into the picture, as seen in preferential oxidation of the methylene groups in 1-methylcyclohexane that are most distant from the methyl substituent.

The lessons from these early experiments have been reinforced, codified, and solidified by a large body of data. Korzekwa and colleagues reported a theoretical study in which semiempirical quantum chemical calculations were used to develop a predictive model for P450 mediated hydroxylations (154). The essential feature of this model is that the intrinsic reactivity of a given C-H bond can be defined by its bond strength, where bond strength is defined as the energy required to break the C-H bond homolytically: C-H -> C· + H·. As the energy of the hydrogen radical is constant for all the reactions, the bond strength is determined by the stability of the carbon radical that is generated in the reaction. In the Korzekwa model, abstraction of the hydrogen by the *p*-nitrosophenoxy radical was found to give the most quantitatively accurate calculated transition state, but the principle is the same: i.e., that the relative reactivities of two C-H bonds can be predicted by their relative bond strengths. As shown by the bond strengths listed in Table 3, this approximation predicts the following order of C-H bond reactivity: benzylic or allylic > tertiary > secondary > primary. Vinylic hydrogens have too high a bond strength to undergo direct hydroxylation. Indeed, as shown by the hepane oxidation results in Figure 18, this is the general order that is observed when C-H bond oxidation is controlled by intrinsic reactivity rather than by steric constraints or positioning of the substrate within the active site.

This conclusion is supported by studies in which the activation energies for hydrogen abstraction by cytochrome P450 were calculated by DFT (160,161). The results yielded a relative order of reactivity consistent with that inferred earlier from the heptane metabolism experiments, i.e., benzylic or allylic > tertiary> secondary > primary.

In a more recent analysis, six different computational methodologies for predicting the site of oxidative metabolism on drug molecules were compared, using a structurally varied set of molecules that are metabolized by CYP3A4 and/or CYP2C9 to validate the predictions (162). Three of the methods (QMBO, QMSpin, SPORCalc) based their prediction entirely on the chemical structure of the substrate in question, two employed structural information on the enzymes catalyzing the oxidation (MetaDock, MetaGlide), and one combined the substrate structure and protein structure approaches (Metasite). The results suggested that the intrinsic reactivity of the C-H bonds was of paramount importance, whereas the structure of the specific enzyme involved in the oxidation was less important than first expected.

4. Conclusions

It is a crucial feature of the scientific method that as progress is made new questions and new approaches arise, some of which reopen earlier conclusions for further study. In the past two

decades, earlier conclusions concerning the nature of the P450 oxidizing species, and the mechanism of its reaction with substrates, have been reexamined in light of new approaches and the emergence of apparent anomalies. This reexamination, and the associated debate, continues, but overall the concurrence of experimental and theoretical results tend to support a refinement of the originally postulated mechanism. This mechanism postulates that the Compound I Por+·Fe(IV)=O species is the primary oxidant in P450 catalysis and that a radical rebound mechanism is the route for insertion of an oxygen atom into the C-H bond of a hydrocarbon.

Acknowledgments

References

1. Guengerich, FP. Cytochrome P450: Structure, Mechanism, and Biochemistry. Ortiz de Montellano, PR., editor. Kluwer Elsevier; New York: 2005. p. 377-530.

2. McLean KJ, Munro AW. Drug Metab Rev 2008;40:427. [PubMed: 18642141]

3. Ehlting J, Provart NJ, Werck-Reichhart D. Biochem Soc Trans 2006;34:1192. [PubMed: 17073783]

4. Schuler MA, Werck-Reichhart D. Annu Rev Plant Biol 2003;54:629. [PubMed: 14503006]

5. Nelson DR, Kamataki T, Waxman DJ, Guengerich FP, Estabrook RW, Feyereisen R, Gonzalez FJ, Coon MJ, Gunsalus IC, Gotoh O, Okuda K, Nebert DW. DNA Cell Biol 1993;12:1. [PubMed: 7678494]

6. Poulos TL, Raag R. FASEB J 1992;6:674. [PubMed: 1537455]

7. Denisov IG, Makris TM, Sligar SG, Schlichting I. Chem Rev 2005;105:2253. [PubMed: 15941214]

8. Nishida CR, Ortiz de Montellano PR. Biochem Biophys Res Commun 2005;338:437. [PubMed: 16139791]

9. Yano JK, Koo LS, Schuller DJ, Li H, Ortiz de Montellano PR, Poulos TL. J Biol Chem 2000;275:31086. [PubMed: 10859321]

10. Parek SY, Yamane K, Adachi S, Shiro Y, Weiss KE, Maves SA, Sligar SG. J Inorg Biochem 2002;91:491–501. [PubMed: 12237217]

11. Oku Y, Ohtaki A, Kamitori S, Nakamura N, Yohda M, Ohno H, Kawarabayashi Y. J Inorg Biochem 2004;98:1194. [PubMed: 15219985]

12. Yano JK, Blasco H, Li H, Schmid RD, Henne A, Poulos TL. J Biol Chem 2003;278:608. [PubMed: 12401810]

13. Ho WW, Li H, Nishida CR, Ortiz de Montellano PR, Poulos TL. Blochemistry 2008;47:2071.

14. Narhi LO, Fulco AJ. J Biol Chem 1987;262:6683. [PubMed: 3106360]

15. Fasan R, Chen MM, Crook NC, Arnold FH. Angew Chem Int Ed 2007;46:8414.

16. Cirino PC, Arnold FH. Curr Opin Chem Biol 2002;6:130. [PubMed: 12038995]

17. Nazor J, Dannenmann S, Adjei RO, Fordjour YB, Ghampson IT, Blanusa M, Roccatano D, Schwaneberg U. Protein Eng Design Selec 2008;21:29.

18. Seifert A, Vomund S, Grohmann K, Kriening S, Urlacher VB, Laschat S, Pleiss J. ChemBioChem 2009;10:853. [PubMed: 19222039]

19. van Vugt-Lussenburg BMA, Stjernschantz E, Lastdrager J, Oostenbrink C, Vermeulen NPE, Commandeur JNM. J Med Chem 2007;50:455. [PubMed: 17266197]

20. Poulos, TL.; Johnson, EF. Cytochrome P450: Structure, Mechanism, and Biochemistry. Ortiz de Montellano, PR., editor. Kluwer Elsevier; New York: 2005. p. 87-114.

21. Dawson JH, Sono M. Chem Rev 1987;87:12155.

22. Sundaramoorthy M, Terner J, Poulos TL. Structure 1995;3:1367. [PubMed: 8747463]

23. Hager LP, Morris DR, Brown FS, Eberwein H. J Biol Chem 1966;241:1769. [PubMed: 5945851]

24. Tanabe T, Ullrich V. J Lipid Mediators Cell Signal 1995;12:243.

25. Matsunaga I, Yamada A, Lee DS, Obayashi E, Fujiwara N, Kobayashi K, Ogura H, Shiro Y. Biochemistry 2002;41:1886. [PubMed: 11827534]

26. Lee DS, Yamada A, Sugimoto H, Matsunaga I, Ogura H, Ichihara K, Adachi S, Park SY, Shiro Y. J Biol Chem 2003;278:9761. [PubMed: 12519760]

27. Puchkaev AV, Wakagi T, Ortiz de Montellano PR. J Am Chem Soc 2002;124:12682. [PubMed: 12392414]

28. Puchkaev AV, Ortiz de Montellano PR. Arch Biochem Biophys 2005;434:169. [PubMed: 15629120]

29. Isin EM, Guengerich FP. Biochim Biophys Acta 2007;1770:314. [PubMed: 17239540]

30. Ortiz de Montellano, PR.; De Voss, JJ. Cytochrome P450: Structure, Mechanism and Biochemistry. Ortiz de Montellano, PR., editor. Kluwer Elsevier; New York: 2005. p. 183-245.

31. Rowland P, Blaney FE, Smyth MG, Jones JJ, Leydon VR, Oxbrow AK, Lewis CJ, Tennant MG, Modi S, Eggleston DS, Chenery RJ, Bridges AM. J Biol Chem 2006;281:7614. [PubMed: 16352597]

32. Guengerich FP, Miller GP, Hanna IH, Saato H, Martin MV. J Biol Chem 2002;277:33711. [PubMed: 12093814]

33. Hannemann F, Bichet A, Ewen KM, Bernhardt R. Biochim Biophys Acta 2007;1770:330. [PubMed: 16978787]

34. Paine, MJI.; Scrutton, NS.; Munro, AW.; Gutierrez, A.; Roberts, GCK.; Wolf, CR. Cytochrome P450: Structure, Function, and Mechanism. 3rd. Ortiz de Montellano, PR., editor. Kluwer Elsevier; New York: 2005. p. 115

35. Murataliev MB, Feyereisen R, Walker A. Biochim Biophys Acta 2004;1698

36. Munro AW, Leys DG, McLean KJ, Marshall KR, Ost TW, Daff S, Miles CS, Chapman SK, Lysek DA, Moser CC, Page CC, Dutton PL. Trends Biochem Sci 2002;27:250. [PubMed: 12076537]

37. Hawkes DB, Adams GW, Burlingame AL, Ortiz de Montellano PR, De Voss JJ. J Biol Chem 2002;277:27725. [PubMed: 12016226]

38. Roberts GA, Çelik A, Hunter DJB, Ost TWB, White JH, Chapman SK, Turner NJ, Flitsch SL. J Biol Chem 2003;278:48914. [PubMed: 14514666]

39. Schlichting I, Berendzen J, Chu K, Stock AM, Maves SA, Benson DE, Sweet RM, Ringe D, Petsko GA, Sligar SG. Science 2000;287:1615. [PubMed: 10698731]

40. Beitlich T, Kuhnel K, Schulze-Briese C, Shoeman RL, Schlichting I. J Synchrotron Radiat 2007;14:11. [PubMed: 17211068]

41. Peterson JA, Ishimura Y, Griffin BW. Arch Biochem Biophys 1972;149:197. [PubMed: 4335959]

42. Bon Hoa GH, Begard E, Debey P, Gunsalus IC. Biochemistry 1978;17:2835. [PubMed: 687565]

43. Denisov IG, Grinkova YV, Baas BJ, Sligar SG. J Biol Chem 2006;281:233313.

44. Grinkova YV, Denisov IG, Waterman MR, Arase M, Kagawa N, Sligar SG. Biochem Biophys Res Commun 2008;372:379. [PubMed: 18482580]

45. Nagano S, Poulos TL. J Biol Chem 2005;280:31659. [PubMed: 15994329]

46. Sharrock M, Debrunner PG, Schultz C, Lipscomb JD, Marshall V, Gunsalus IC. Biochim Biophys Acta 1976;420:8. [PubMed: 2296]

47. Sono M, Perera R, Jin S, Makris TM, Sligar SG, Bryson TA, Dawson JH. Arch Biochem Biophys 2005;436:40. [PubMed: 15752707]

48. Dawson JH, Kau LS, Penner-Hahn JE, Sono M, Eble KS, Bruce GS, Hager LP, Hodgson KO. J Am Chem Soc 1986;108:8114.

49. Hu S, Schenider AJ, Kincaid MR. J Am Chem Soc 1991;113:4815.

50. Macdonald IDG, Sligar SG, Christian JF, Unno M, Champion PM. J Am Chem Soc 1999;121:376.

51. Harris D, Loew G, Waskell L. J Am Chem Soc 1998;120:4308.

52. Wang D, Zheng J, Shaik S, Thiel W. J Phys Chem B 2008;112:5126. [PubMed: 18386859]

53. Wang D, Thiel W. J Molec Struct Theochem 2009;898:90.

54. Makris, TM.; Denisov, I.; Schlichting, I.; Sligar, SG. Cytochrome P450: Structure, Function, and Mechanism. 3rd. Ortiz de Montellano, PR., editor. Kluwer Elsevier; New York: 2005. p. 149

55. Davydov R, Kappl R, Hütterman J, Peterson JA. FEBS Lett 1991;295:113. [PubMed: 1662641]

56. Davydov R, Macdonald IDG, Makris TM, Sligar SG, Hoffman BM. J Am Chem Soc 1999;121:10654.

57. Mak PJ, Denisov IG, Victoria D, Makris TM, Deng T, Sligar SG, Kincaid JR. J Am Chem Soc 2007;129:6382. [PubMed: 17461587]

58. Davydov R, Chemerisov S, Werst DE, Rajh T, Matsui T, Ikeda-Saito M, Hoffman BM. J Am Chem Soc 2004;126:15960. [PubMed: 15584719]

59. Makris TM, von Koenig K, Schlichting I, Sligar SG. Biochemistry 2007;46:14129. [PubMed: 18001135]

60. Davydov R, Makris TM, Kofman V, Werst DE, Sligar SG, Hoffman BM. J Am Chem Soc 2001;123:1403. [PubMed: 11456714]

61. Denisov IG, Makris TM, Sligar SG. J Biol Chem 2001;276:11648. [PubMed: 11152470]

62. Denisov IG, Hung SC, Weiss KE, McLean MA, Shiro Y, Park SY, Champion PM, Sligar SG. J Inorg Biochem 2001;87:215. [PubMed: 11744059]

63. Davydov R, Perera R, Jin S, Yang TC, Bryson TA, Sono M, Dawson JH, Hoffman BM. J Am Chem Soc 2005;127:1403. [PubMed: 15686372]

64. Tajima K, Edo T, Ishizu K, Imaoka S, Funae Y, Oka S, Sakurai H. Biochem Biophys Res Commun 1993;191:157. [PubMed: 8383486]

65. Rahimtula AD, O'Brien PJ, Hrycay EG, Peterson JA, Estabrook RW. Biochem Biophys Res Commun 1974;60:695. [PubMed: 4371068]

66. Blake RC, Coon MJ. J Biol Chem 1981;256:5755. [PubMed: 7240170]

67. Wagner GC, Palcic MM, Dunford HB. FEBS Lett 1983;156:244. [PubMed: 6852258]

68. Schünemann V, Jung C, Trautwein AX, Mandon D, Weiss R. FEBS Lett 2000;179:149.

69. Schünemann V, Jung C, Terner J, Trautwein AX, Weiss R. J Inorg Biochem 2002;91:586. [PubMed: 12237224]

70. Schünemann V, Lendzian F, Jung C, Contzen J, Barra AL, Sligar SG, Trautwein AX. J Biol Chem 2004;279:10919. [PubMed: 14688245]

71. Jung C, Schünemann V, Lendzian F. Biochem Biophys Res Commun 2005;338:355. [PubMed: 16143295]

72. Prasad S, Mitra S. Biochem Biophys Res Commun 2004;314:610. [PubMed: 14733951]

73. Egawa T, Shimada H, Ishimura Y. Biochem Biophys Res Commun 1994;201:1464. [PubMed: 8024592]

74. Spolitak T, Dawson JH, Ballou DP. J Biol Chem 2005;280:20300. [PubMed: 15781454]

75. Kellner DG, Hung SC, Weiss KE, Sligar SG. J Biol Chem 2002;277:9641. [PubMed: 11799104]

76. Spolitak T, Dawson JH, Ballou DP. J Biol Inorg Chem 2008;13:599. [PubMed: 18273651]

77. Gustafsson JA, Rondahl L, Bergman J. Biochemistry 1979;18:865. [PubMed: 420819]

78. Hrycay EG, Gustafsson JA, Ingelman-Sundberg M, Ernster L. Biochem Biophys Res Commun 1975;66:209. [PubMed: 240357]

79. Danielsson H, Wikvall K. FEBS Lett 1976;66:299. [PubMed: 8336]

80. Gustafsson JA, Hrycay EG, Ernster L. Arch Biochem Biophys 1976;174:440. [PubMed: 180899]

81. Hrycay EG, Gustafsson JA, Ingelman-Sundberg M, Ernster L. Eur J Biochem 1976;61:43. [PubMed: 173555]

82. Kexel, H.; Schmelz, E.; Schmidt, HL. Microsomes and Drug Oxidations. Ullrich, V.; Roots, I.; Hildebrandt, A.; Estabrook, RW.; Conney, AH., editors. Pergamon Press; Elmsford, N.Y.: 1977. p. 269-274.

83. Heimbrook DC, Sligar SG. Biochem Biophys Res Commun 1981;99:530. [PubMed: 7236281]

84. Macdonald TL, Burka LT, Wright ST, Guengerich FP. Biochem Biophys Res Commun 1982;104:620. [PubMed: 6803786]

85. Nam W, Valentine JS. J Am Chem Soc 1993;115:1772.

86. Bhakta MN, Hollenberg PF, Wimalasena K. J Am Chem Soc 2005;127:1376. [PubMed: 15686361]

87. Kim SJ, Latifi R, Ang HY, Nam W, de Visser SP. Chem Commun 2009:1562.

88. Zhang R, Chandrasena REP, Martinez E II, Horner JH, Newcomb M. Org Lett 2005;7:1193. [PubMed: 15760172]

89. Harischandra DN, Zhang R, Newcomb M. J Am Chem Soc 2005;127:13776. [PubMed: 16201783]

90. Pan Z, Zhang R, Fung LWM, Newcomb M. Inorg Chem 2007;46:1517. [PubMed: 17284026]

91. Pan Z, Wang Q, Sheng X, Horner JH, Newcomb M. J Am Chem Soc 2009;131:2621. [PubMed: 19193008]

92. Altun A, Shaik S, Thiel W. J Am Chem Soc 2007;129:8978. [PubMed: 17595079]

93. Shaik S, Cohen S, Wang Y, Chen H, Kumar D, Thiel W. Chem Rev. 2009 in press.

94. Newcomb M, Zhang R, Chandrasena REP, Halgrimson JA, Horner JH, Makris TM, Sligar SG. J Am Chem Soc 2006;128:4580. [PubMed: 16594688]

95. Behan RK, Hoffart LM, Stone KL, Krebs C, Green MT. J Am Chem Soc 2007;129:5855. [PubMed: 17432853]

96. Newcomb M, Halgrimson JA, Horner JH, Wasinger EC, Chen LX, Sligar SG. Proc Natl Acad Sci USA 2008;105:8179. [PubMed: 18174331]

97. Alvarez B, Radi R. Amino Acids 2003;25:295. [PubMed: 14661092]

98. Sheng X, Zhang H, Im SC, Horner JH, Waskell L, Hollenberg PF, Newcomb M. J Am Chem Soc 2009;131:2971. [PubMed: 19209859]

99. Sheng X, Horner JH, Newcomb M. J Am Chem Soc 2008;130:13310. [PubMed: 18788736]

100. Bergstrom S, Lindstredt S, Samuelson B, Corey EJ, Gregoriou GA. J Am Chem Soc 1958;80:2337.

101. Corey EJ, Gregoriou GA, Peterson DH. J Am Chem Soc 1958;80:2338.

102. Shapiro S, Piper JU, Caspi E. J Am Chem Soc 1982;104:2301.

103. Fretz H, Woggon WD, Voges R. Helv Chim Acta 1989;72:391.

104. Groves JT, McClusky GA, White RE, Coon MJ. Biochem Biophys Res Commun 1978;81:154. [PubMed: 656092]

105. White RE, Miller JP, Favreau LV, Bhattacharyaa A. J Am Chem Soc 1986;108:6024.

106. Krauser JA, Guengerich FP. J Biol Chem 2005;280:19496. [PubMed: 15772082]

107. Iyer KR, Jones JP, Darbyshire JF, Trager WF. Biochemistry 1997;36:7136. [PubMed: 9188713]

108. Harrelson JP, Henne KR, Alonso DOV, Nelson SD. Biochem Biophys Res Commun 2007;352:843. [PubMed: 17156750]

109. Anderson C, Iyer KR, Jones JP, Darbyshire JF, Trager WF. J Am Chem Soc 1999;121:4.

110. Harrelson JP, Atkins WM, Nelson SD. Biochemistry 2008;47:2978. [PubMed: 18247580]

111. Sheng X, Zhang H, Hollenberg PF, Newcomb M. Biochemistry 2009;48:1620. [PubMed: 19182902]

112. Gelb MH, Heimbrook DC, Mälkönen P, Sligar SG. Biochemistry 1982;21:370. [PubMed: 7074020]

113. Fourneron JD, Archelas A, Furstoss R. J Org Chem 1989;54:2478.

114. Tanaka K, Kurihara N, Nakajima M. Pestic Biochem Physiol 1979;10:79.

115. Groves JT, Subramanian DV. J Am Chem Soc 1984;106:2177.

116. Oliw EH, Brodowsky ID, Hörnsten L, Hamberg M. Arch Biochem Biophys 1993;300:434. [PubMed: 8424677]

117. McClanahan RH, Huitric AC, Pearson PG, Desper JC, Nelson SD. J Am Chem Soc 1988;110:1979.

118. Stanjek V, Miksch M, Lueer P, Matern U, Boland W. Angew Chem Int Ed 1999;38:400.

119. Larbat R, Kellner S, Specker S, Hehn A, Gontier E, Hans J, Bourgaud F, Matern U. J Biol Chem 2007;282:542. [PubMed: 17068340]

120. Larbat R, Hehn A, Hans J, Schneider S, Jugdé H, Schneider B, Matern U, Bourgaud F. J Biol Chem 2009;284:4776. [PubMed: 19098286]

121. Bowry VW, Ingold KU. J Am Chem Soc 1991;113:5699.

122. Newcomb M, Manek MB, Glenn AG. J Am Chem Soc 1991;113:949.

123. Ortiz de Montellano PR, Stearns RA. J Am Chem Soc 1987;109:3415.

124. Newcomb M, Manek MB, Glenn AG. J Am Chem Soc 1991;113:949.

125. Bach RD, Schlegel HB, Andrés JL, Sosa C. J Am Chem Soc 1994;116:3475.

126. Auclair K, Hu Z, Little DM, Ortiz de Montellano PR, Groves JT. J Am Chem Soc 2002;124:6020. [PubMed: 12022835]

127. Newcomb M, Shen R, Lu Y, Coon MJ, Hollenberg PF, Kopp DA, Lippard SJ. J Am Chem Soc 2002;124:6879. [PubMed: 12059209]

128. Newcomb M, Shen R, Lu Y, Coon MJ, Hollenberg PF, Kopp DA, Lippard SJ. J Am Chem Soc 2006;128:1394.

129. He X, Ortiz de Montellano PR. J Biol Chem 2004;279:39479. [PubMed: 15258138]

130. Jiang Y, He X, Ortiz de Montellano PR. Biochemistry 2006;45:533. [PubMed: 16401082]

131. Newcomb M, Shen R, Choi SY, Toy PH, Hollenberg PF, Vaz ADN, Coon MJ. J Am Chem Soc 2000;122:2677.

132. Cryle MJ, Stuthe JMU, Ortiz de Montellano PR, De Voss JJ. Chem Commun 2004:512.

133. Cryle MJ, Ortiz de Montellano PR, DeVoss JJ. J Org Chem 2005;70:2455. [PubMed: 15787531]

134. Atkinson JK, Ingold KU. J Am Chem Soc 1993;32:9209.

135. Toy PH, Newcomb M, Hollenberg PF. J Am Chem Soc 1998;120:7719.

136. Newcomb M, Le Tadic MH, Putt DA, Hollenberg PF. J Am Chem Soc 1995;117:3313.

137. Rettie AE, Rettenmeier AW, Howald WN, Baillie TA. Science 1987;235:890. [PubMed: 3101178]

138. Rettie AE, Boberg M, Rettenmeier AW, Baillie TA. J Biol Chem 1988;263:13733. [PubMed: 3138238]

139. Porubeck DJ, Barnes H, Meier GP, Theodore LJ, Baillie TA. Chem Res Toxicol 1989;2:35. [PubMed: 2519229]

140. Kassahun K, Baillie TA. Drug Metab Dispos 1993;21:242. [PubMed: 8097692]

141. Fisher MB, Thompson SJ, Ribeiro V, Lechner MC, Rettie AE. Arch Biochem Biophys 1998;356:63. [PubMed: 9681992]

142. Rettie AE, Sheffels PR, Korzekwa KR, Gonzalez FJ, Philpot RM, Baillie TA. Biochemistry 1995;34:7889. [PubMed: 7794900]

143. Bell SG, Xu F, Forward I, Bartlam M, Rao Z, Wong LK. J Mol Biol 2008;383:561. [PubMed: 18762195]

144. Höld KM, Sirisoma NS, Casida JE. Chem Res Toxicol 2001;14:589. [PubMed: 11368559]

145. Obach RS. Drug Metab Dispos 2001;29:1599. [PubMed: 11717179]

146. Korzekwa KR, Trager WF, Nagata K, Parkinson A, Gillette JR. Drug Metab Dispos 1990;18:974. [PubMed: 1981547]

147. Vyas KP, Kari PH, Prakash SR, Duggan DE. Drug Metab Dispos 1990;18:218. [PubMed: 1971576]

148. Guan X, Fisher MB, Lang DH, Zheng YM, Koop DR, Rettie AE. Chemico-Biol Interact 1998;110:103.

149. White RE, McCarthy MB. Arch, Biochem Biophys 1986;246:19. [PubMed: 3963820]

150. Hansch C, Zhang L. Drug Metab Rev 1993;25:1. [PubMed: 8449144]

151. Lewis DFV, Jacobs MN, Dickins M. Drug Discovery Today 2004;9:530. [PubMed: 15183161]

152. Cornell NW, Sinclair JF, Stegeman JJ, Hansch C. Alcohol and Alcoholism 1987:251. [PubMed: 3620000]

153. Frommer U, Ullrich V, Staudinger H. Hoppe-Seylers Z Physiol Chem 1970;351:903. [PubMed: 4393760]

154. Korzekwa KR, Jones JP, Gillette JR. J Am Chem Soc 1990;112:7042.

155. Blanksby SJ, Ellison GB. Acc Chem Res 2003;36:255. [PubMed: 12693923]

156. Pratt DA, Mills JH, Porter NA. J Am Chem Soc 2003;125:5801. [PubMed: 12733921]

157. Chandra AK, Uchimaru T, Urata S, Sugie M, Sekiya A. Int J Chem Kinetics 2003;35:130.

158. Korth HG, Sickling W. J Chem Soc Perkin Trans 2 1997:715.

159. van Scheppingen W, Dorrestijn E, Arends I, Mulder P. J Phys Chem A 1997;101:5404.

160. Olsen L, Rydberg P, Rod TH, Ryde U. J Med Chem 2006;49:6489. [PubMed: 17064067]

161. de Visser SP, Kumar D, Cohen S, Shacham R, Shaik S. J Am Chem Soc 2004;126:8362. [PubMed: 15237977]

162. Afzelius L, Arnby CH, Broo A, Carlsson L, Isaksson C, Jurva U, Kjellander B, Kolmodin K, Nilsson K, Raubacher F, Weidolf L. Drug Metab Rev 2007;39:61. [PubMed: 17364881]

Biography

Paul R. Ortiz de Montellano received a BS degree from MIT and MS and PhD degrees from Harvard University for work with E. J. Corey and Konrad Bloch. After a postdoctoral year as a NATO Fellow with Duilio Arigoni at the ETH in Zürich, he spent two years with Syntex before joining the faculty of the Department of Pharmaceutical Chemistry at the University of California, San Francisco. He has research interests at the interface of chemistry and biology, with a particular focus on cytochrome P450 and other hemoproteins.
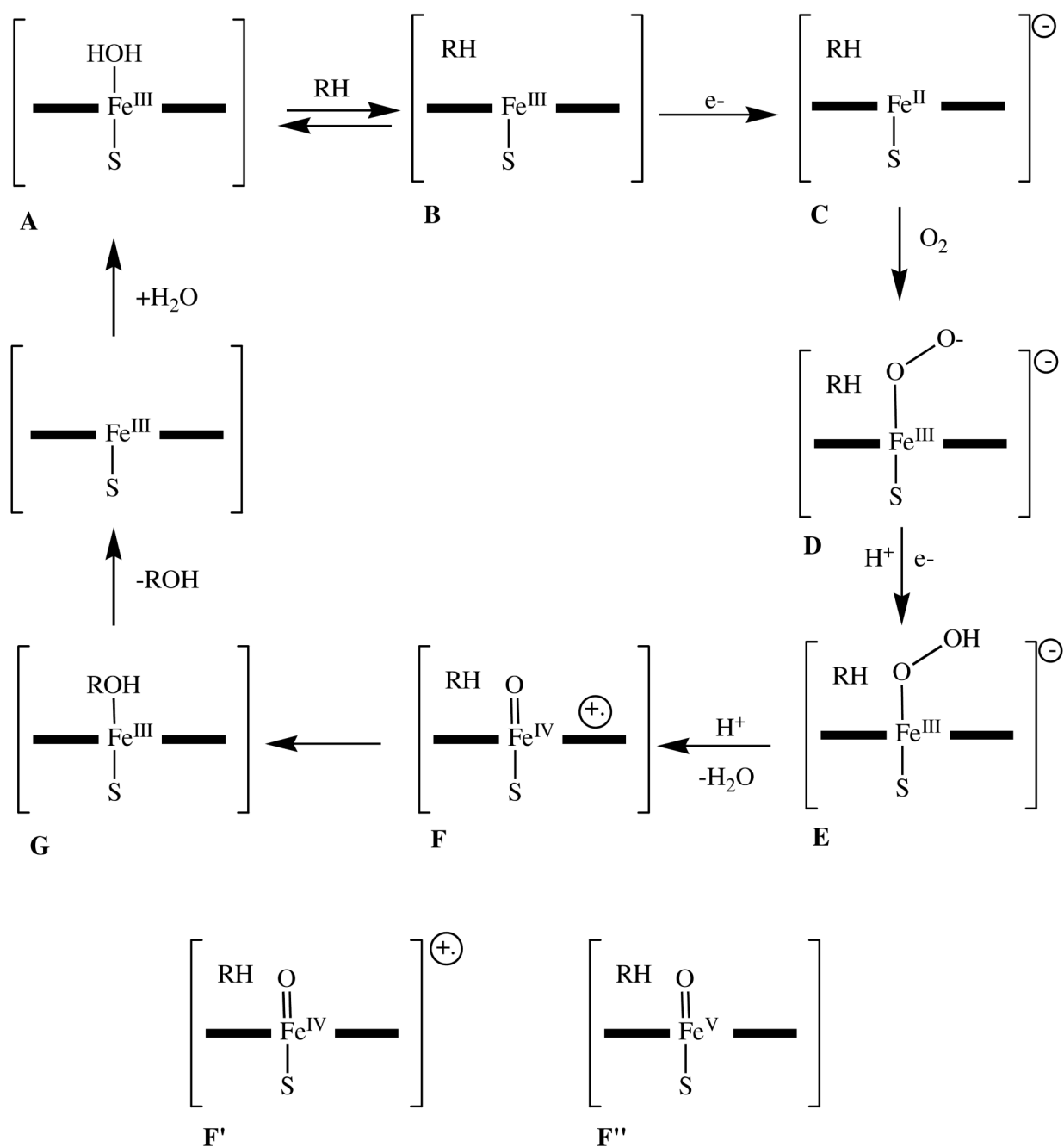
Figure 1.
Summary of the cytochrome P450 catalytic cycle. The heme group is represented as two solid bars with the iron (Fe) between them. The cysteine thiolate provided by the protein is represented as an S. RH is a substrate hydrocarbon and ROH the resulting hydroxylated product. The +· over one of the heme bars indicates the radical cation is located on the porphyrins, whereas its placement besides the brackets indicates that the radical is located somewhere on the protein.
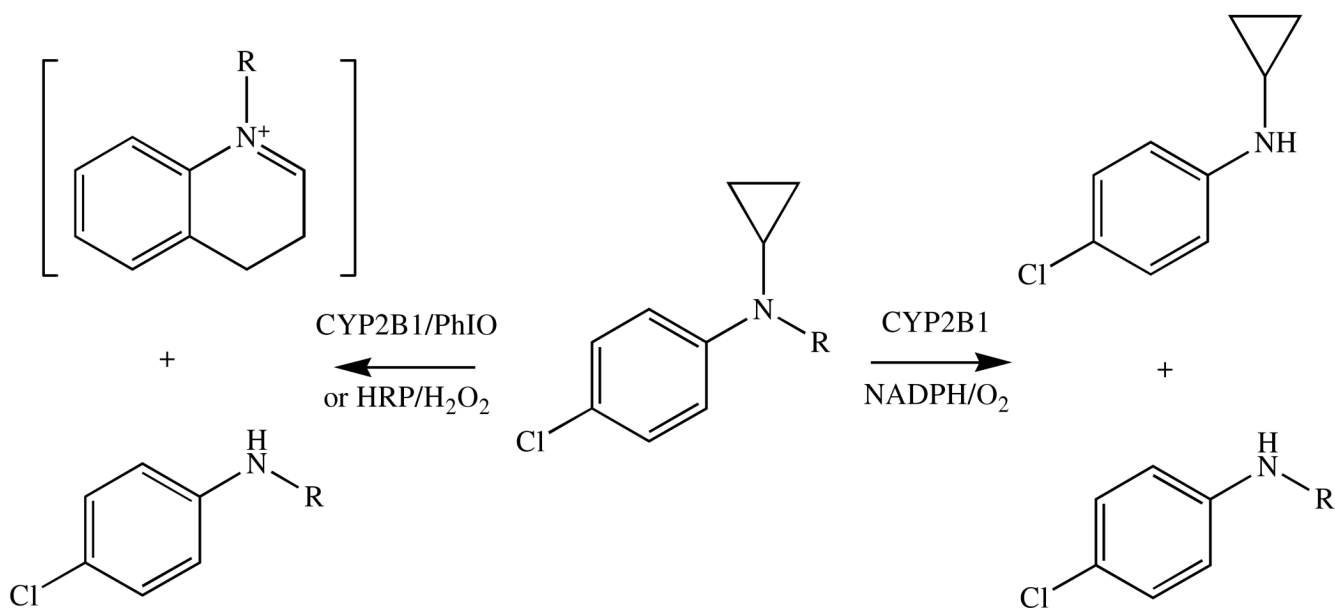
Figure 2.
Comparison of the products from the oxidation of N-alkyl-N-cyclopropyl-*p*-chloroaniline by
CYP2B1 supported by cytochrome P450 reductase, NADPH, and O_2 with the primary products
obtained when the oxidation is mediated by either horseradish peroxidase and H_2O_2 or by
CYP2B1 and PhIO. The charged product shown in brackets is identified after it is trapped by
cyanide ion.
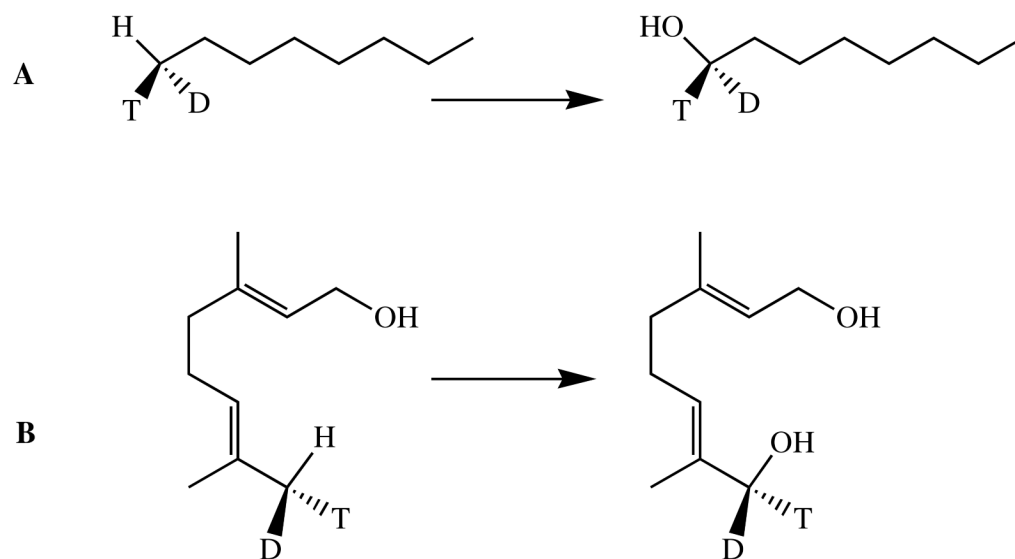
Figure 3.
Retention of stereochemistry in the hydroxylation of terminal methyl groups by cytochrome P450 enzymes.
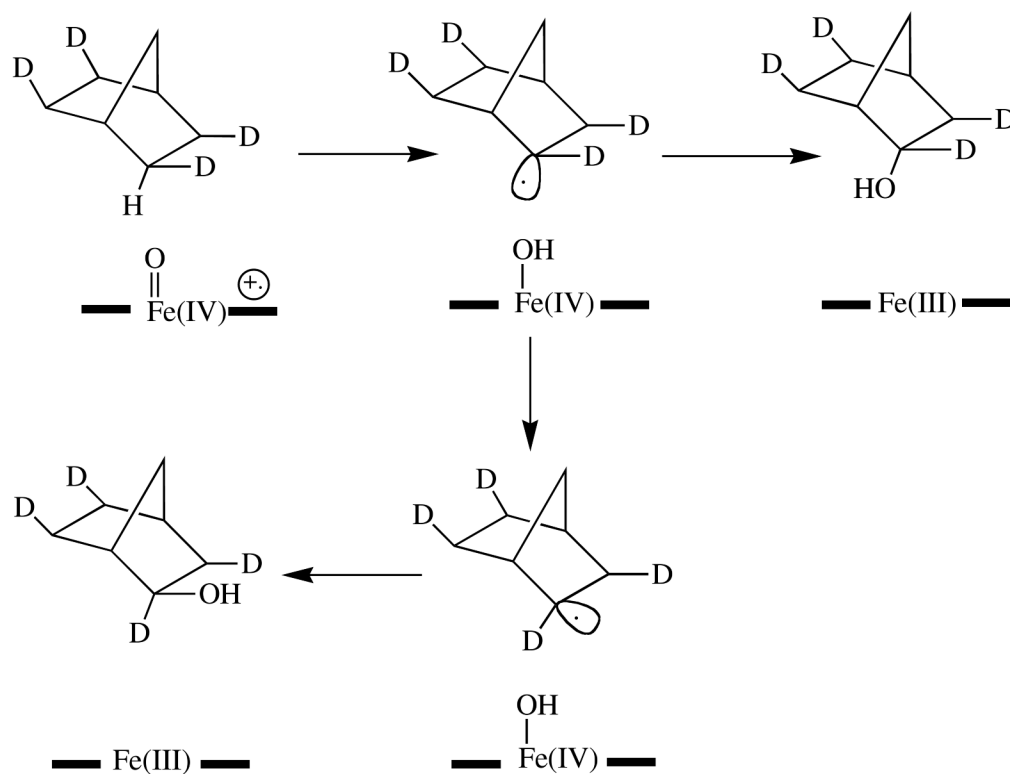
Figure 4.
The cytochrome P450-catalyzed hydroxylation of 2,3,5,6-tetradeuterated norbornane proceeds with partial invertion of stereochemistry at the carbon undergoing hydroxylation, implicating an intermediate such as a radical in the reaction mechanism.
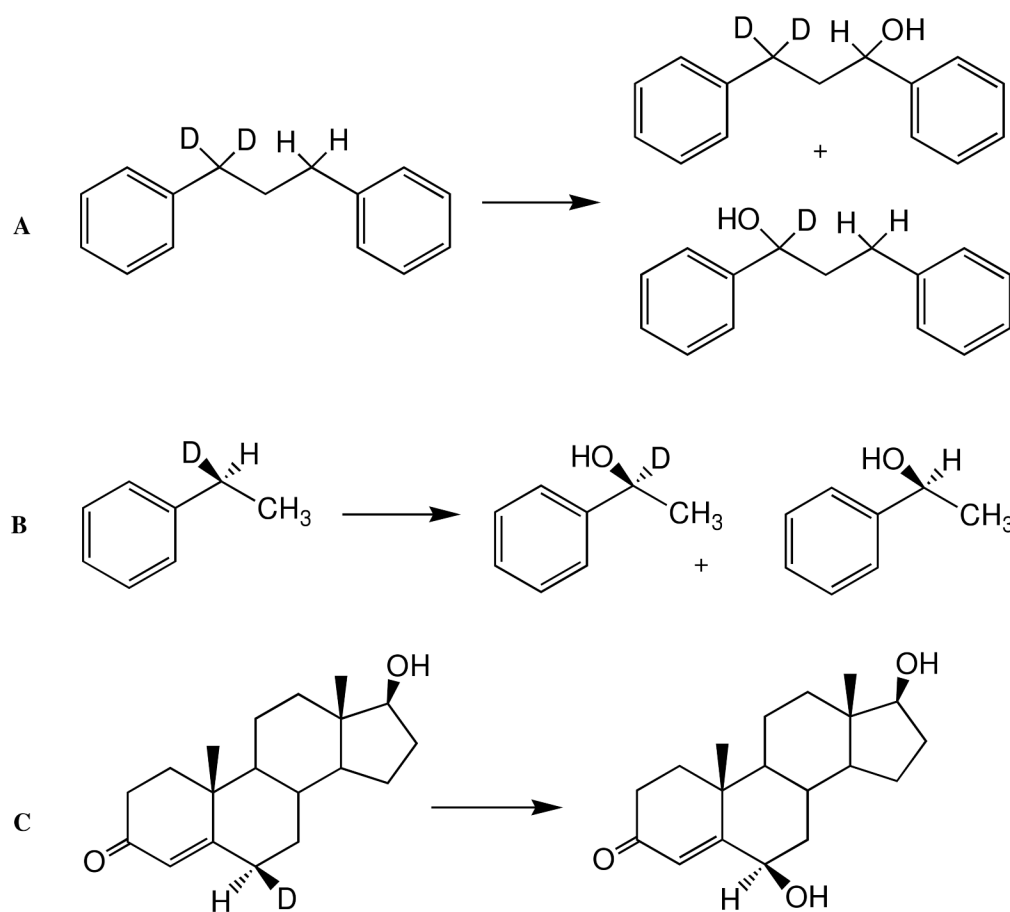
Figure 5.
Selected reactions in which deuterium isotope effects have been used to investigate the nature of cytochrome P450 catalysis.
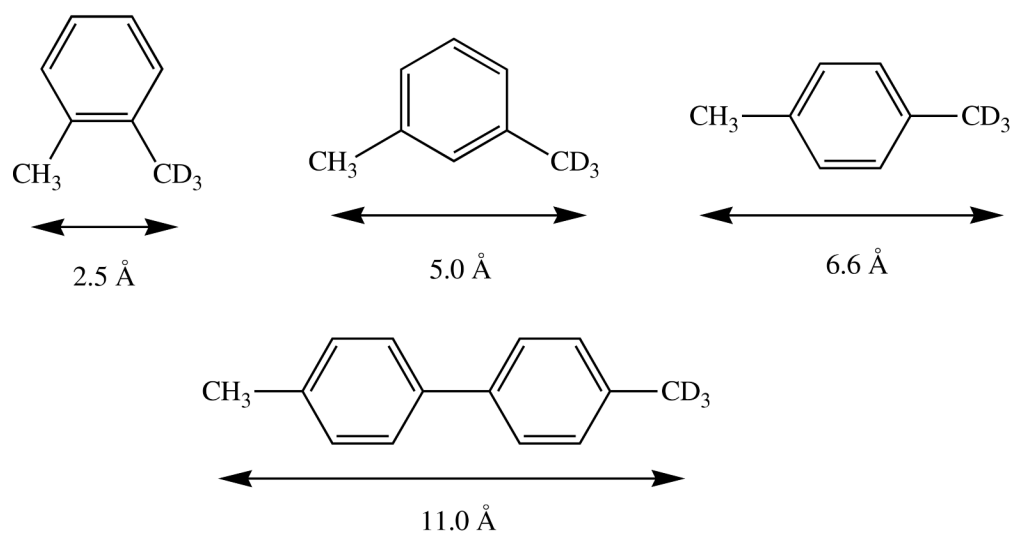
Figure 6.
Low mobility of a substrate within the P450 active site can result in masking of the intrinsic isotope effect in a hydroxylation reaction. The isotope effects observed in the product distributions from hydroxylation of the CH_3 versus CD_3 methyl group in the compounds in this figure depend on the distance between the two groups on the substrate. The distance is indicated in the figure.
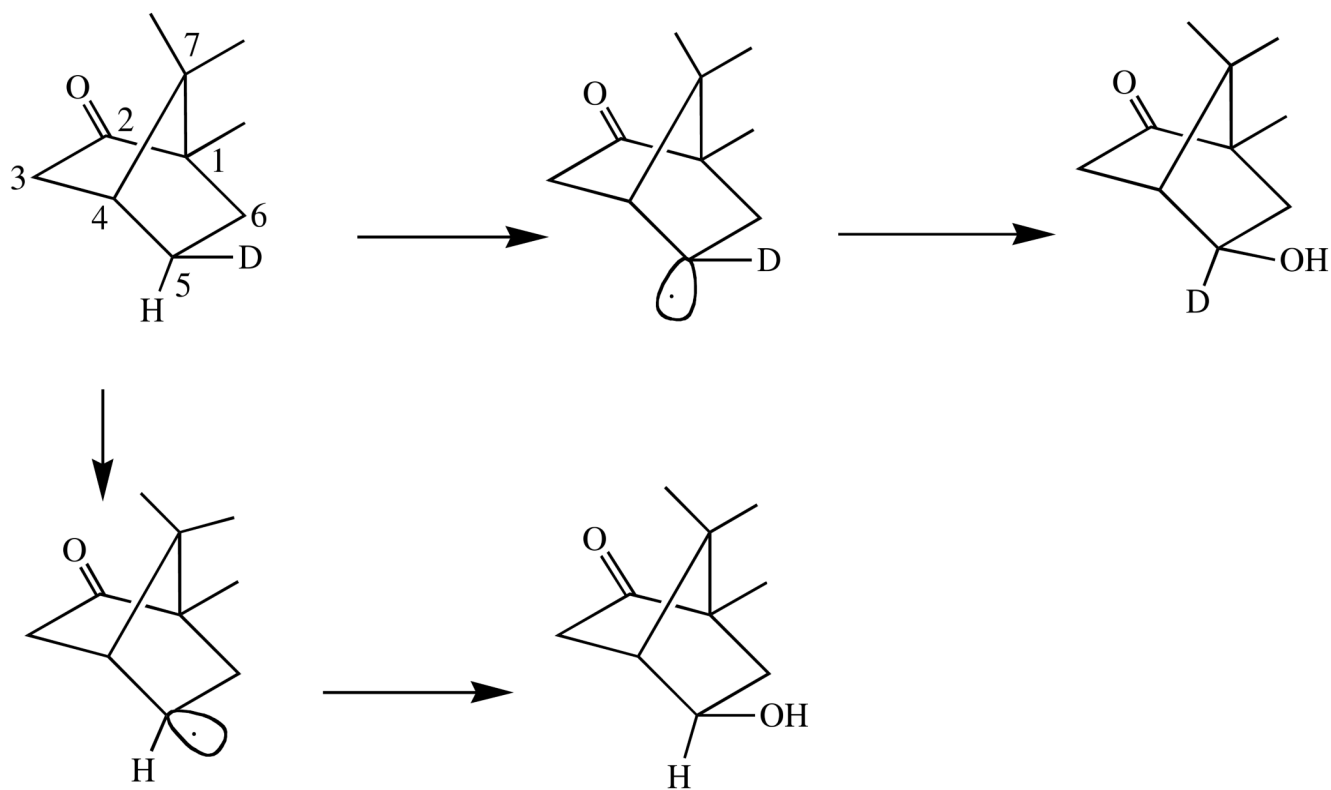
Figure 7.
Inversion of stereochemistry in the hydroxylation of 5-*exo*-deuterated camphor by CYP101.
The carbon atoms are numbered. *Exo* indicates the hydroxyl is on the same side of the molecule
as the bridge with the highest numbered carbon.
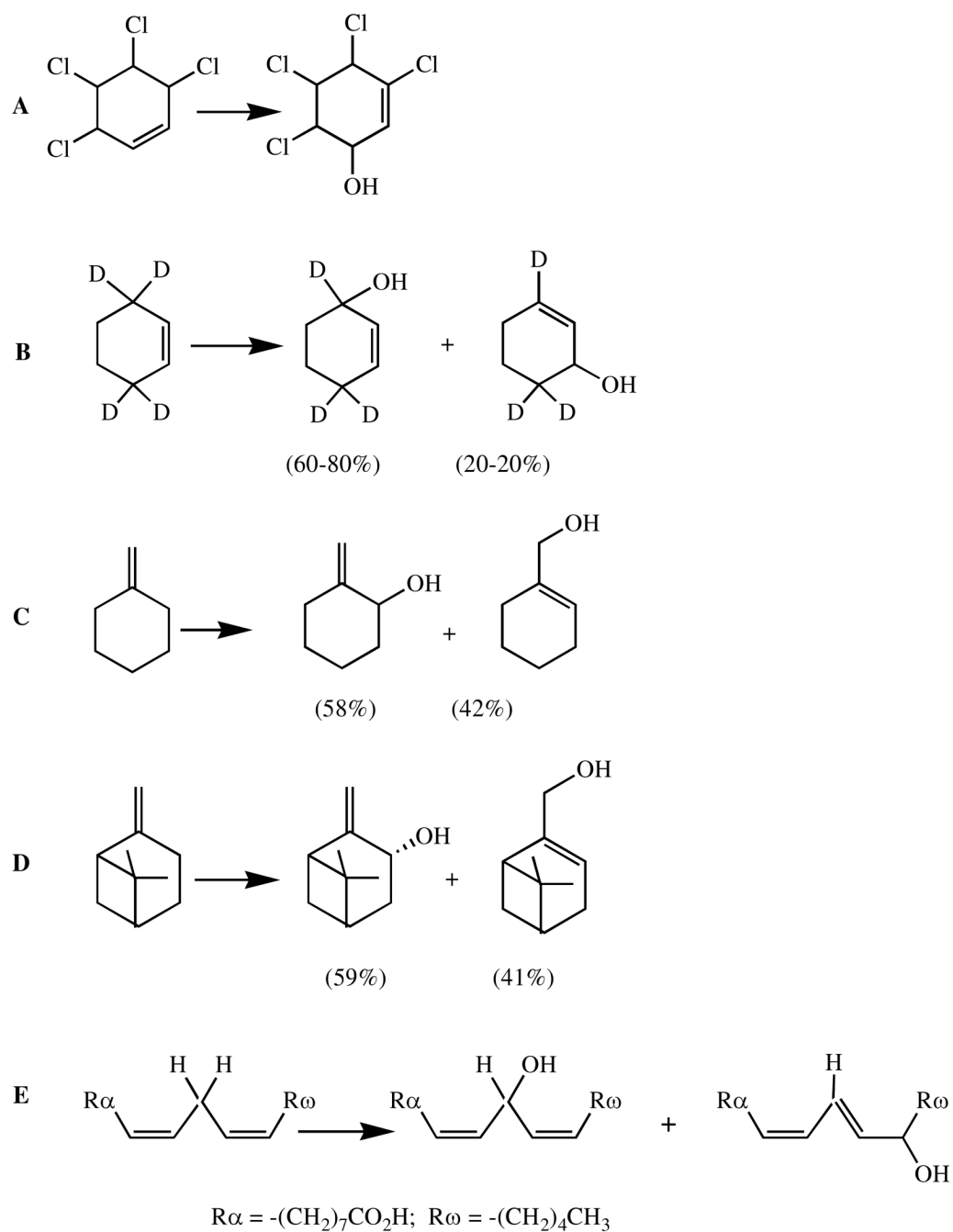
Figure 8.
Reactions in which the hydroxylation regiochemistry is altered due to shift of a double bond allylic to the site from which the hydrogen is removed.
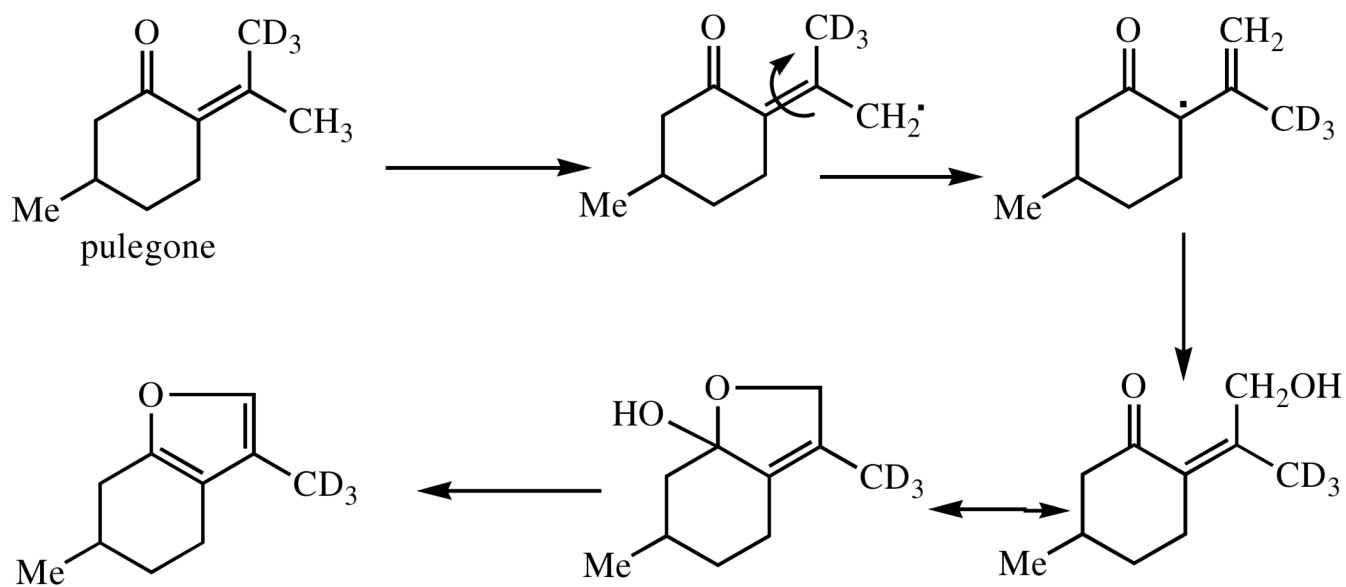
Figure 9.
Loss of stereochemistry observed in the hydroxylation of pulegone by a cytochrome P450 enzyme.
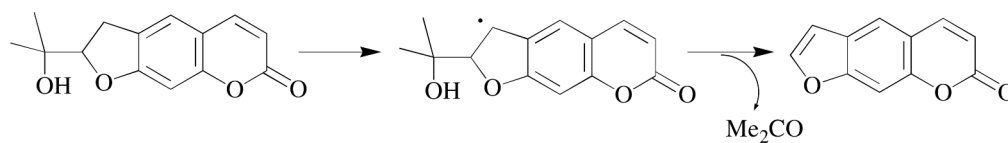
Figure 10.
Cleavage of a carbon-carbon bond in the oxidation of marmesin by cytochrome P450 is best rationalized as occurring from the carbon radical generated by hydrogen abstraction from the dihydrofuran ring of the substrate.
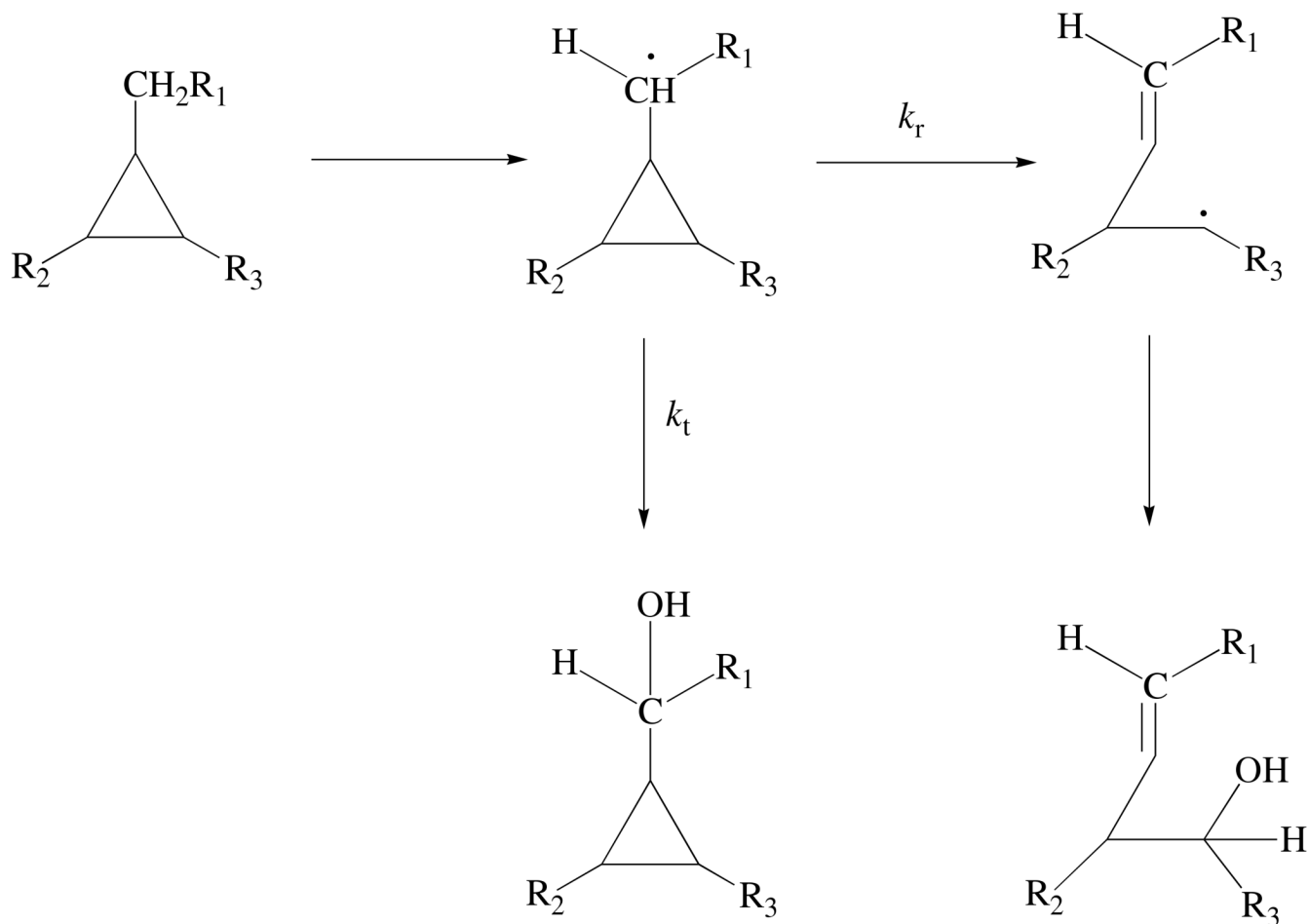
Figure 11.
Schematic of a radical clock reaction manifold. The rate k_t can be estimated from the ratio of the unrearranged and rearranged products if the rate k_r is known (assuming single state reactivity).
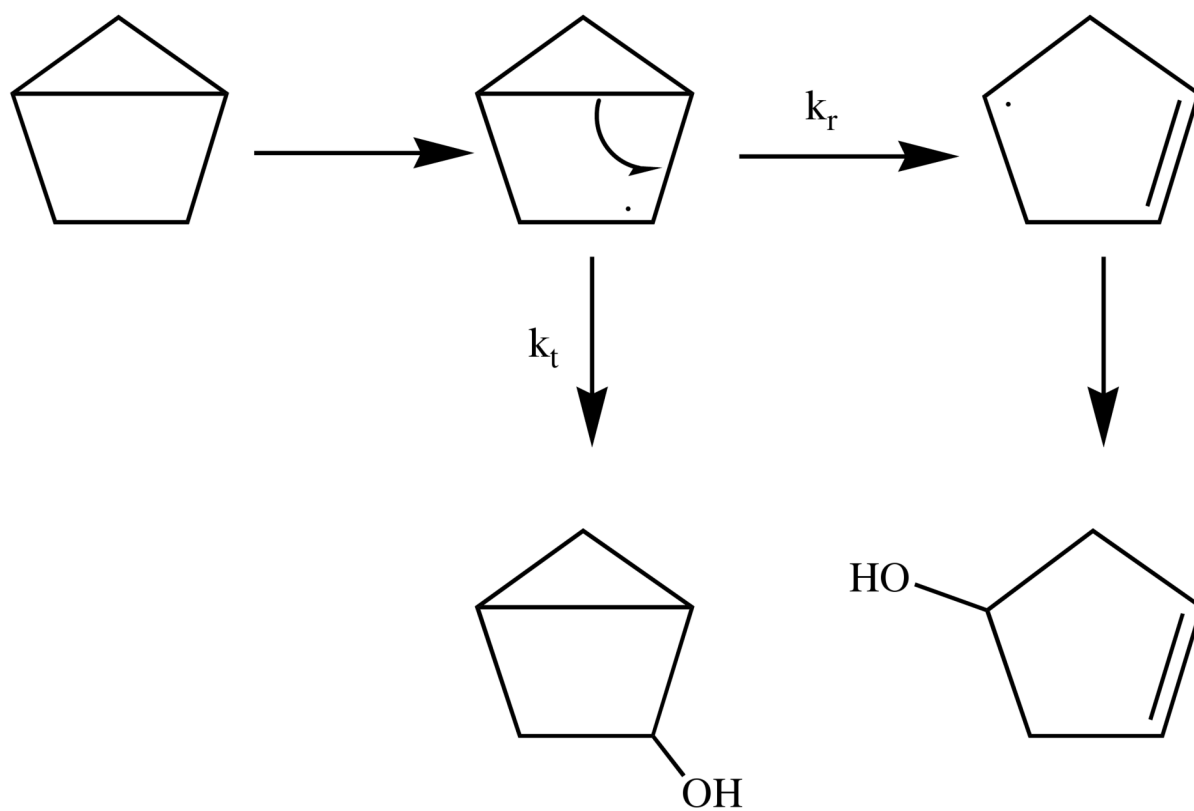
Figure 12.
The oxidation of bicyclo[2.1.0]pentane, a radical clock substrate, by cytochrome P450 yields both a rearranged and an unrearranged hydroxylated product.
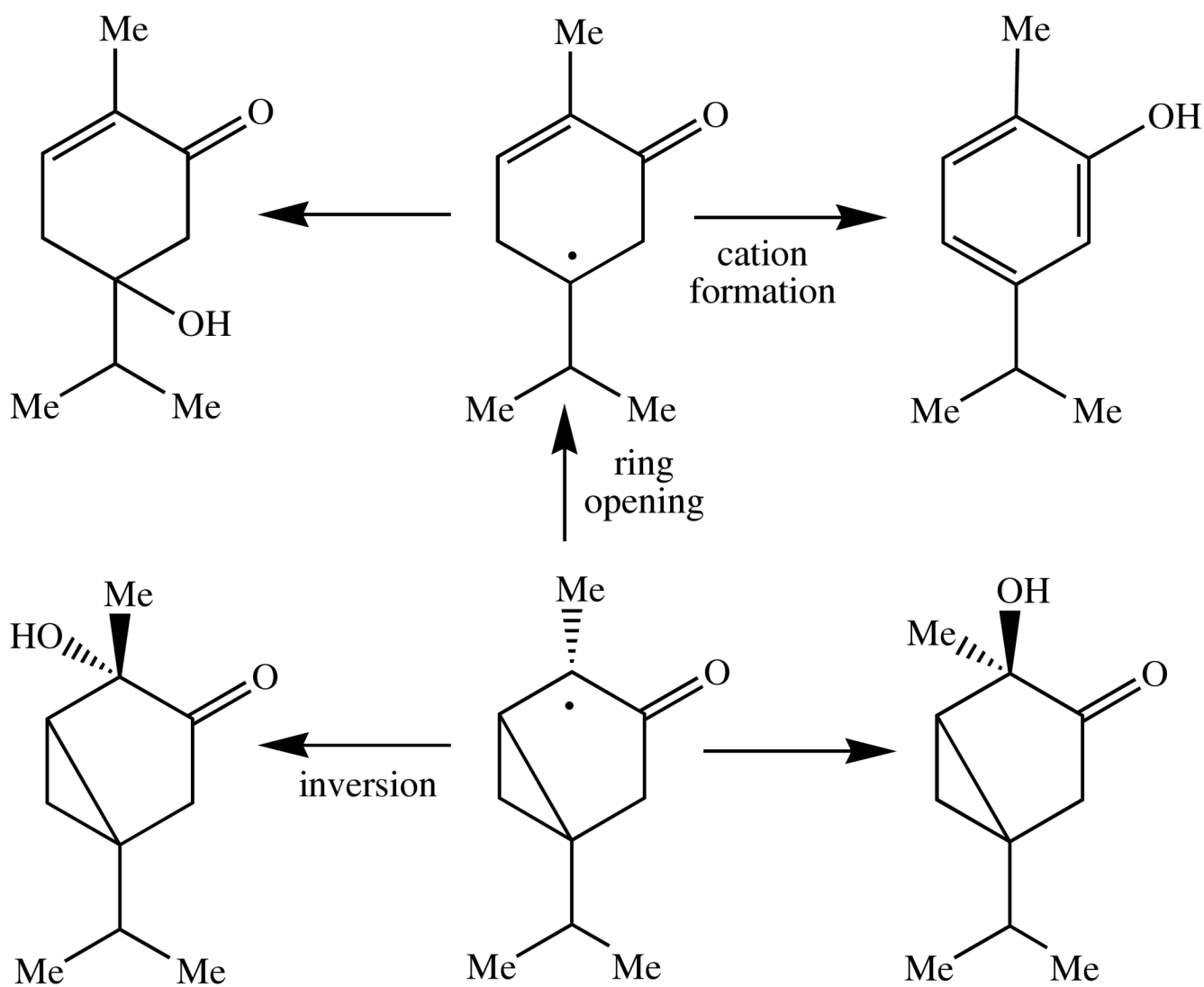
Figure 13.
α- and β-Thujone are radical clocks whose C-4 radical can undergo two simultaneous, competing rearrangements, one a conventional cyclopropyl ring opening reaction and the other an inversion of the stereochemistry of a methyl group. The radical can also be converted to a cation which rearranges to a distinct product.
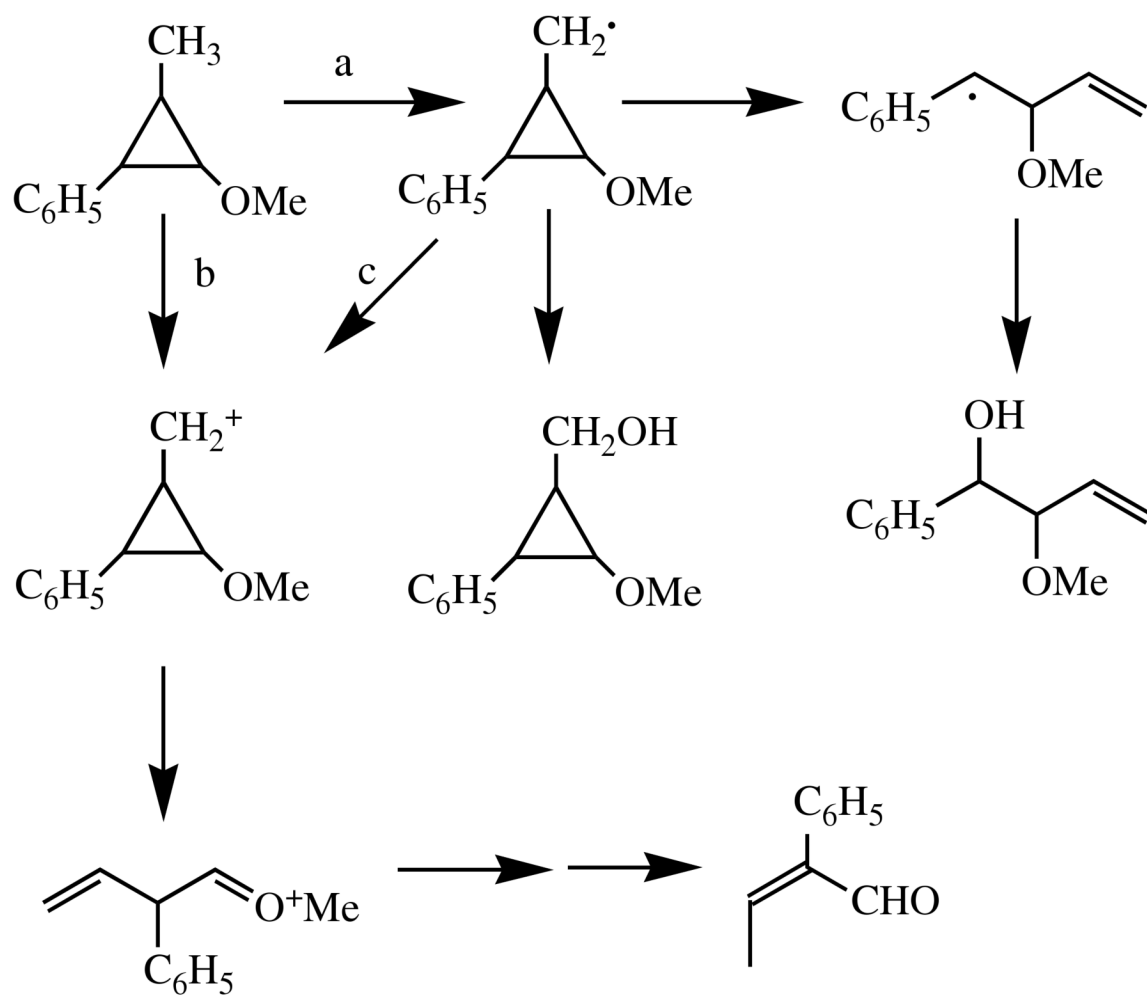
Figure 14.
Rearrangements of a probe that gives different products depending on whether the intermediate is a radical or a cation.
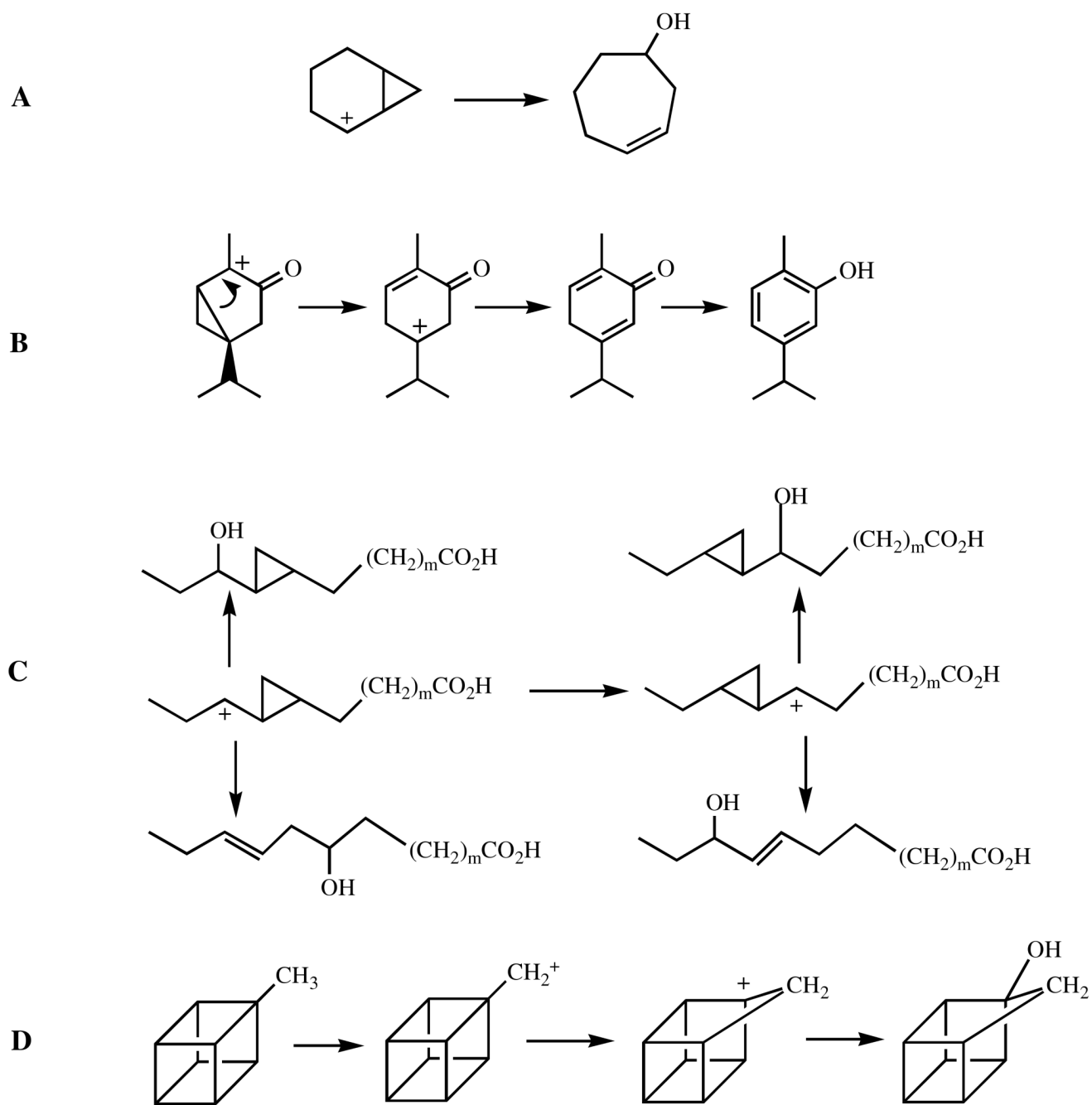
Figure 15.
Rearrangements of various cations used to test for cation involvement in cytochrome P450 hydrocarbon oxidations.
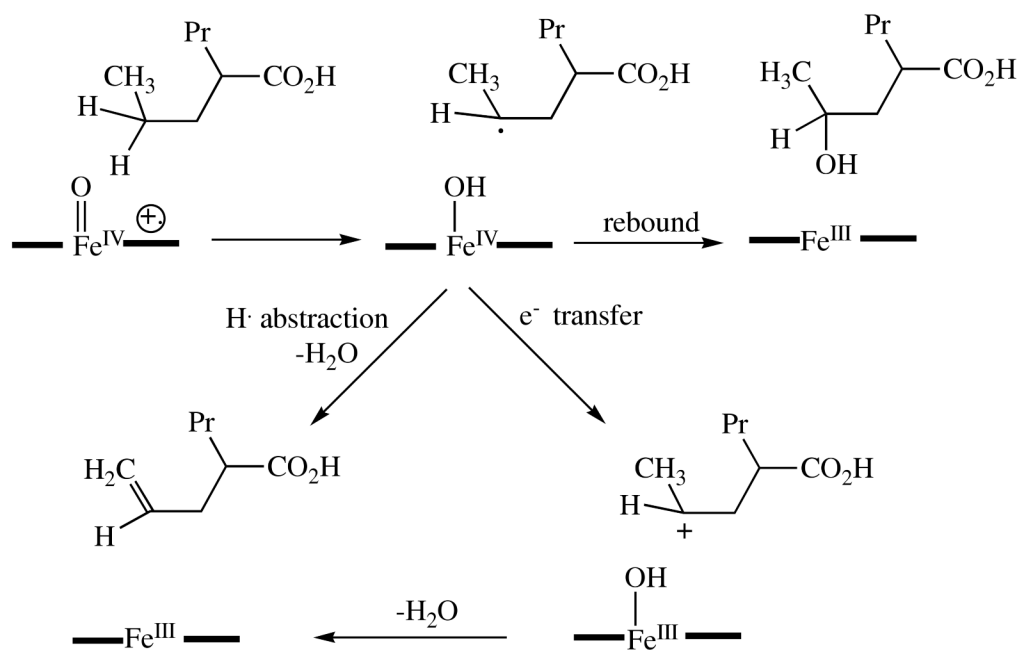
Figure 16.
Desaturatoin of valproic acid via either a cation intermediate or two sequential hydrogen abstraction reactions. The heme is again represented as an iron atom between two black bars.
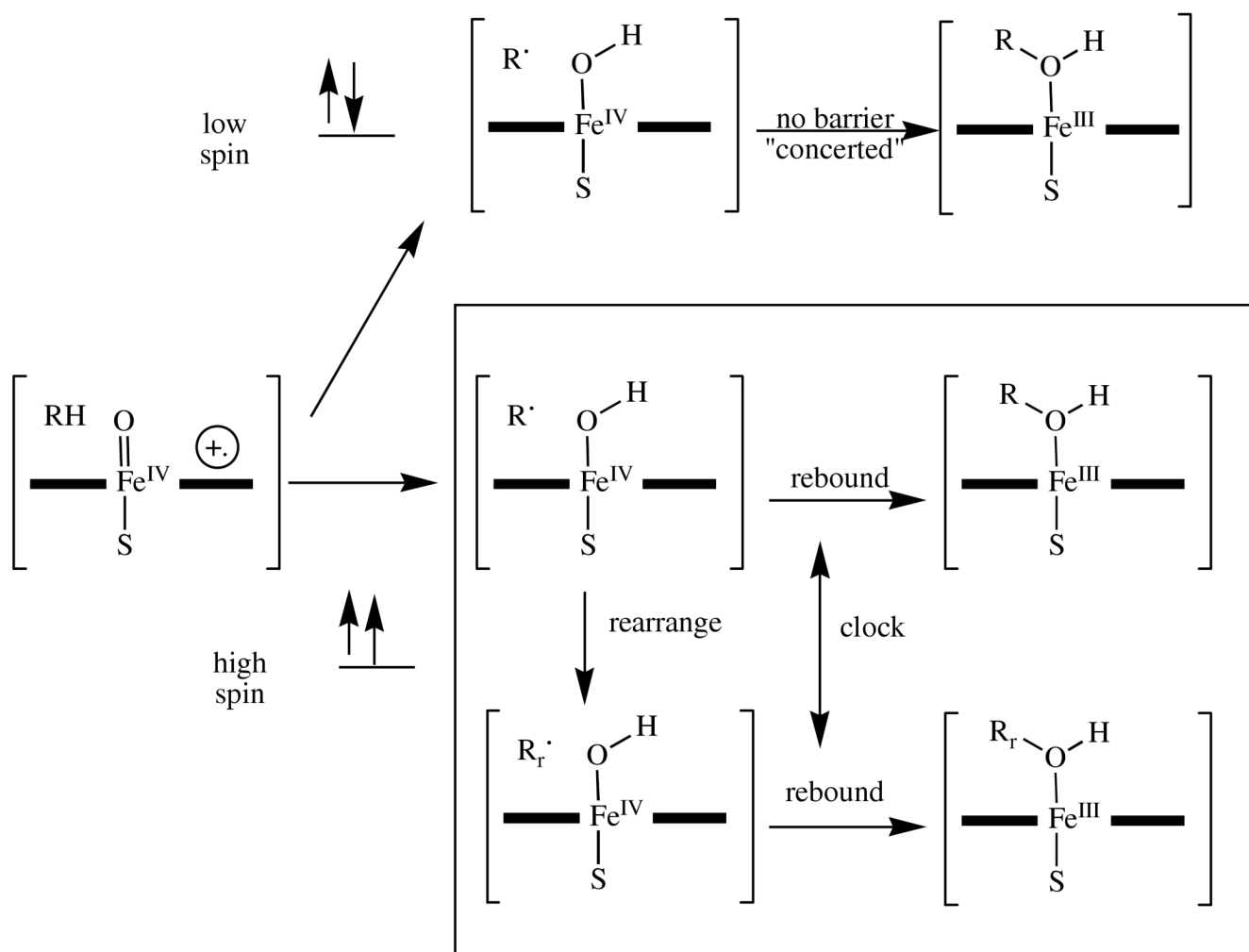
Figure 17.
A schematic showing the rationalization for the observation of extremely fast radical recombination times with some radical clock substrates provided by the two-state hydroxylation hypothesis. The doublet (low) spin transition state collapses in a barrierless manner and is not able to undergo radical rearrangements, whereas the quartet (high) spin transition state (in the box) has a barrier to the recombination reaction that allows the radical rearrangement to occur. The radical clock thus only operates in the lower (high spin) trajectory, but the overall product ratios reflect the sum of the two pathways. As a result, the final product ratio has a deceptively large proportion of the unrearranged product.
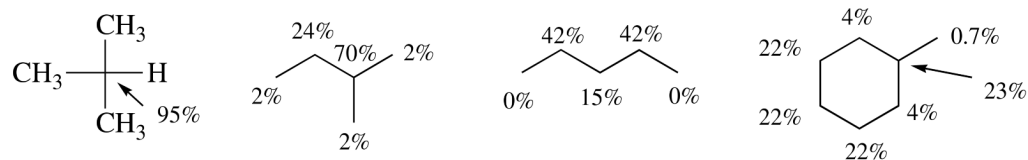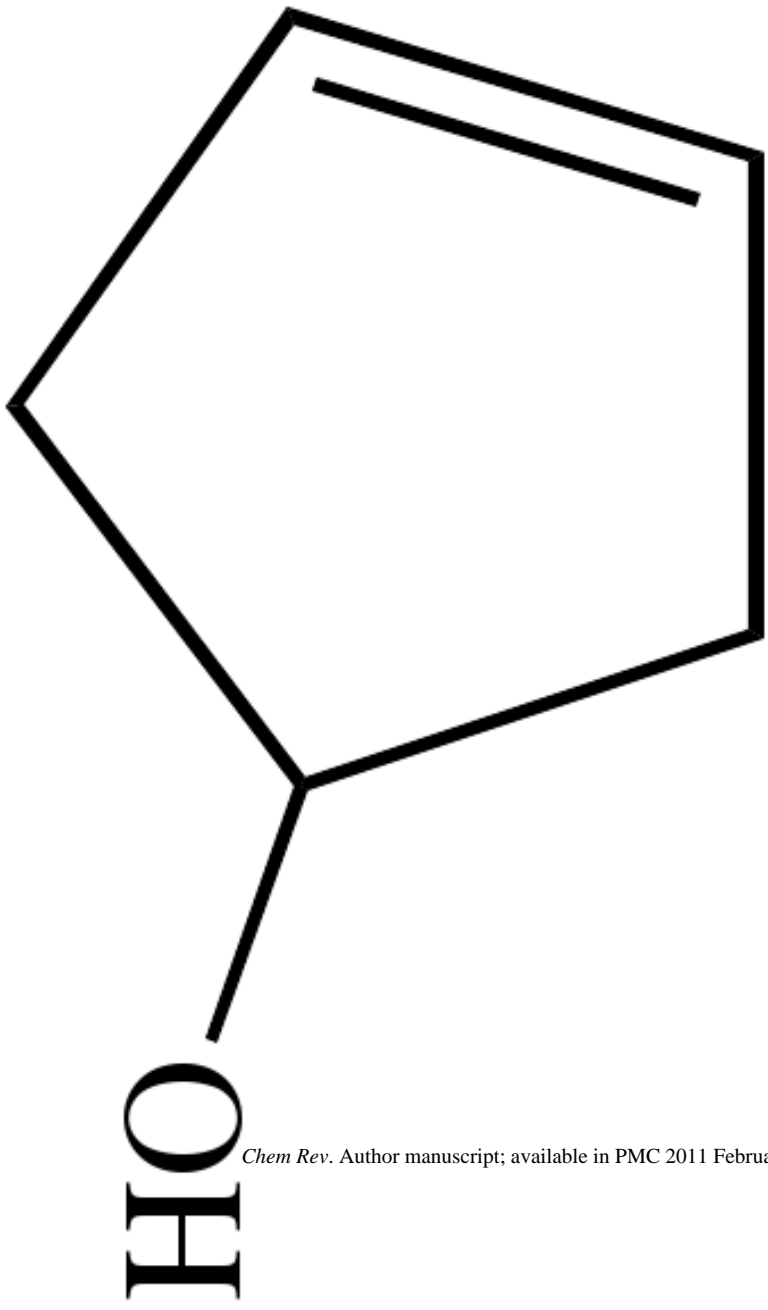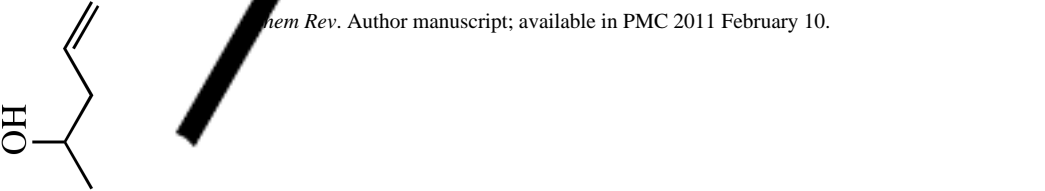
Figure 18.
Sites of hydroxylation of small hydrocarbons by liver microsomal cytochrome P450. The percent of hydroxylation at each site is shown. In the case of equivalent sites, the total hydroxylation at those sites has been divided equally among them.
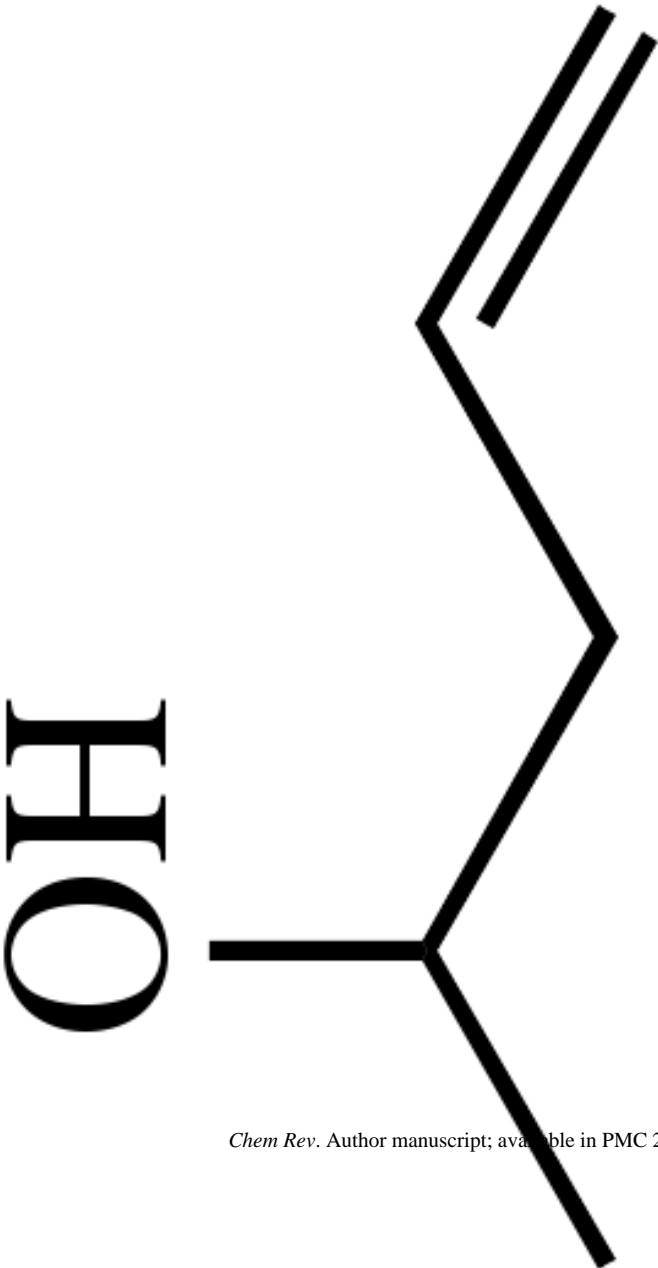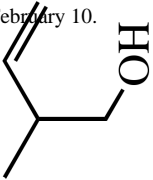
duct, the rate of the
he reference(s) to the
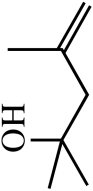
Rearranged product	k_r (s^{-1})	P450 system	k_t (s^{-1})	ref
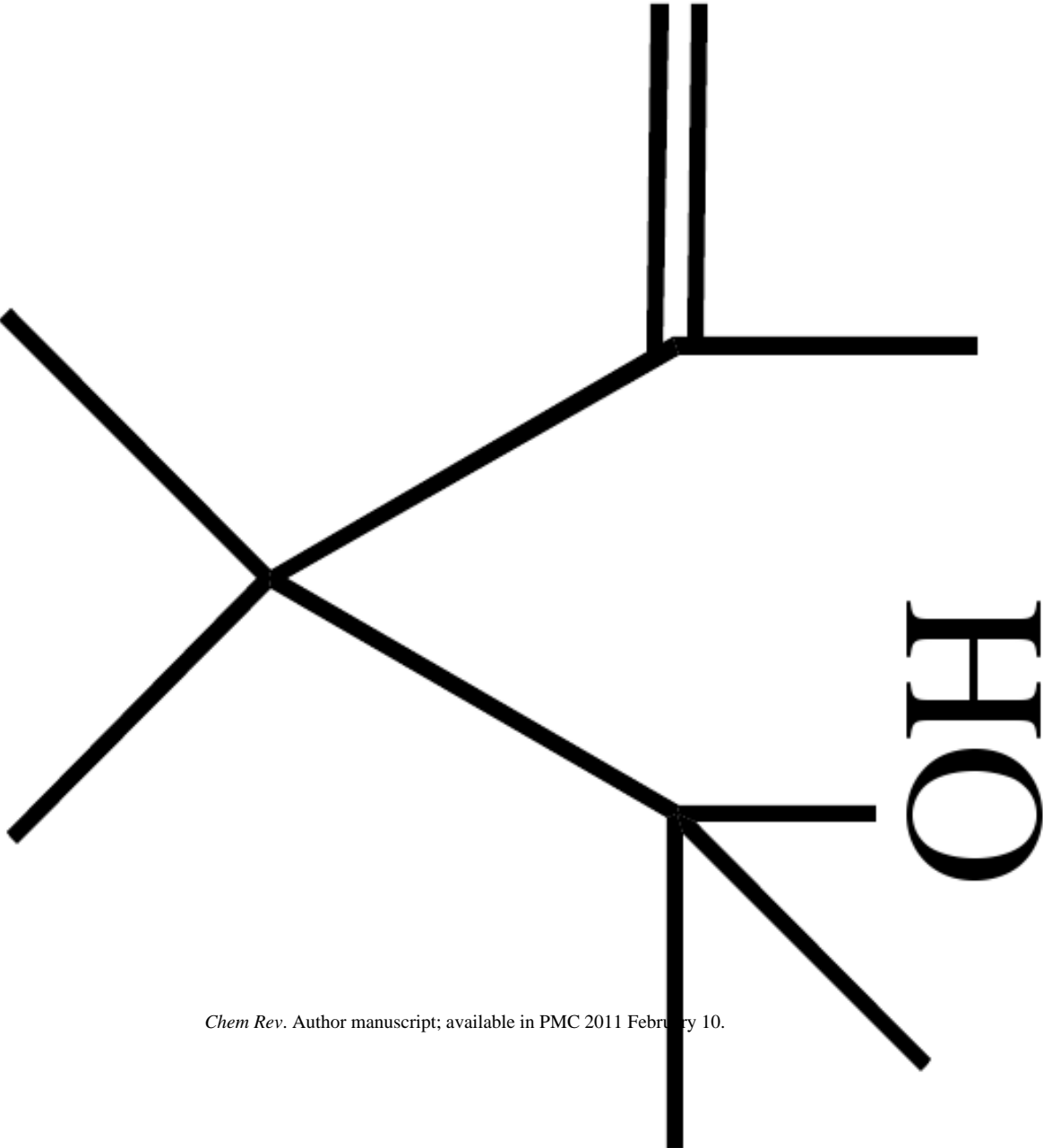
Rearranged product	k_r (s^{-1})	P450 system	k_t (s^{-1})	ref
	2.1×10^9	Rat liver microsomes	2.2×10^{10}	121,123
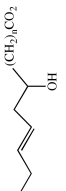
Rearranged product	k_r (s^{-1})	P450 system	k_t (s^{-1})	ref
ND	1.2×10^8	Rat liver microsomes	ND	123
ND	0.8×10^8	Rat liver microsomes	ND	121
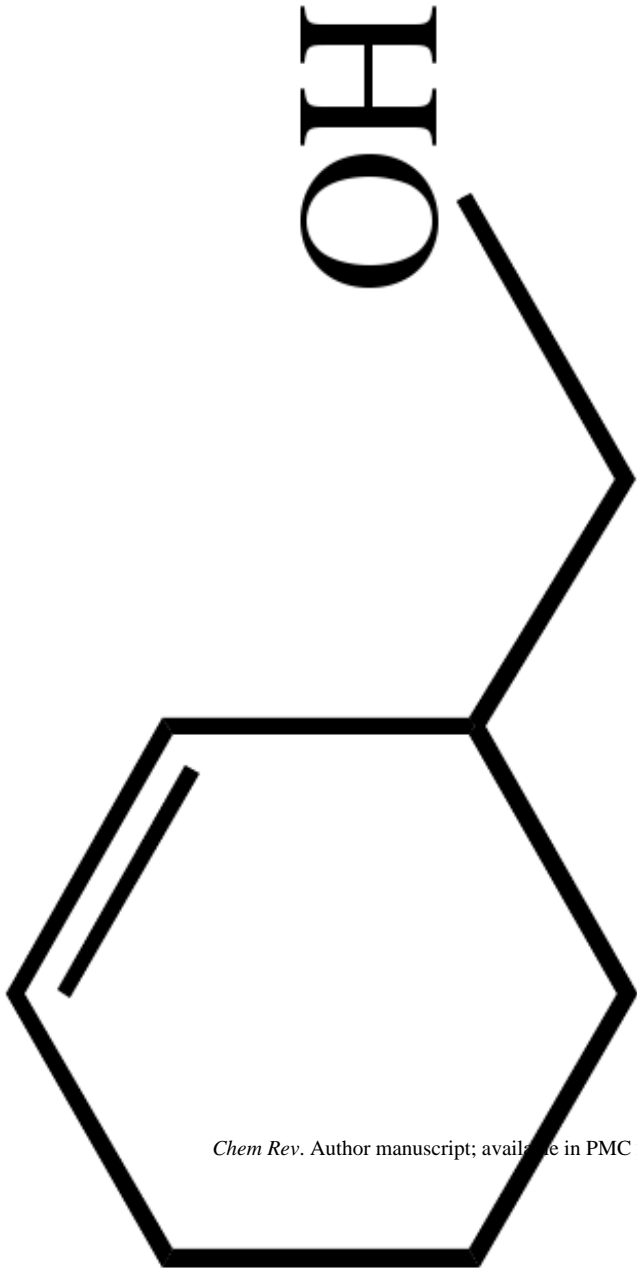
Rearranged product	k_r (s^{-1})	P450 system	k_t (s^{-1})	ref
	1.6×10^8	Rat liver microsomes	1.5×10^{10}	121
	1.8×10^8		1.6×10^{10}	

Rearranged product	k_r (s^{-1})	P450 system	k_t (s^{-1})	ref
	8.0×10^8	Rat liver microsomes	1.9×10^{10}	121
	2.3×10^8		1.8×10^{10}	

Rearranged product	k_r (s^{-1})	P450 system	k_t (s^{-1})	ref
	20×10^8	Rat liver microsomes	2.5×10^{11}	121
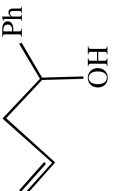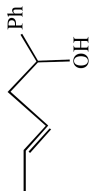
Rearranged product	k_r (s^{-1})	P450 system	k_t (s^{-1})	ref
	47×10^8	Rat liver microsomes, CYP2B4	2.3×10^{11}	134
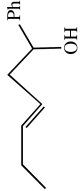
Rearranged product	k_r (s^{-1})	P450 system	k_t (s^{-1})	ref
	8.0×10^8	CYP102	2.6×10^{10}	132,133,
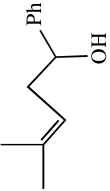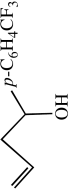
Rearranged product	k_r (s⁻¹)	P450 system	k_t (s⁻¹)	ref
	2×10^8	CYP101, CYP102, CYP2B1, CYP2E1, CYP2B4	$\sim 2 \times 10^{10}$	126,127,128
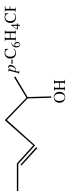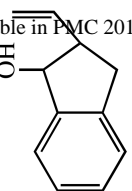
Rearranged product	k_r (s^{-1})	P450 system	k_t (s^{-1})	ref
ND	$<1 \times 10^6$	Rat liver microsomes	ND	121
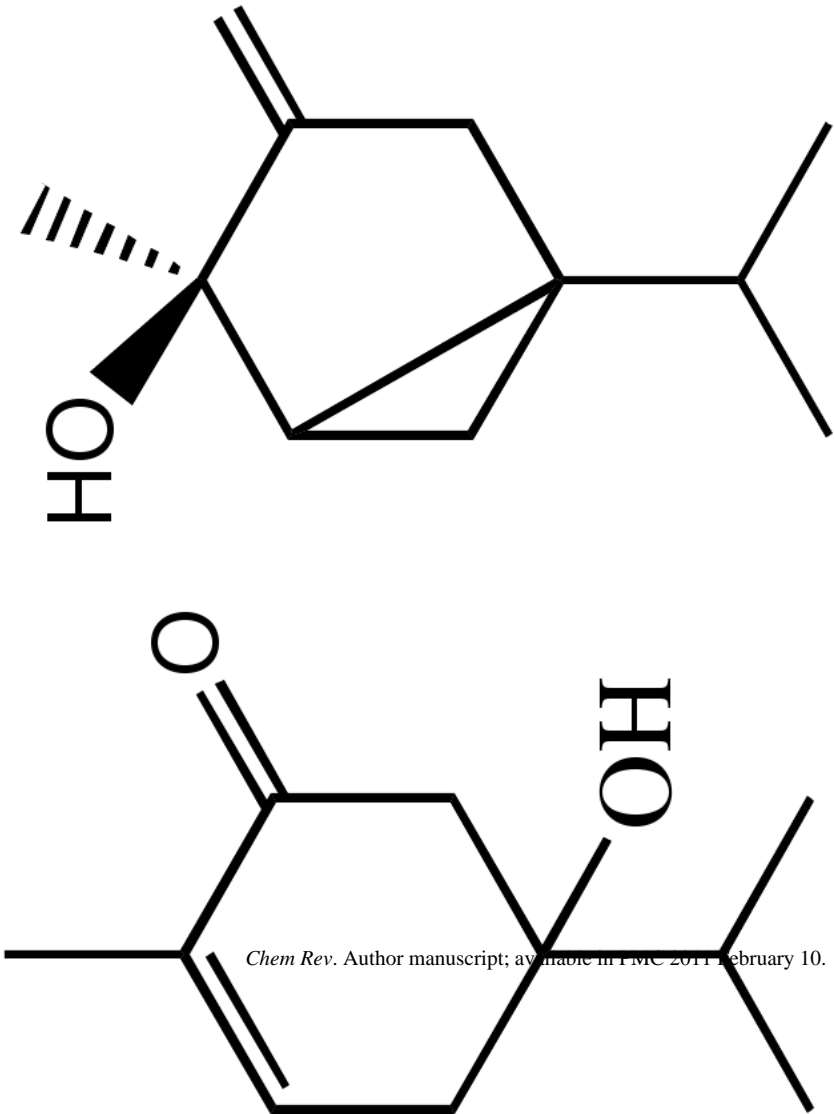
Rearranged product	k_r (s^{-1})	P450 system	k_t (s^{-1})	ref
	5×10^{11}	Rat liver microsomes, CYP2B4	7×10^9 to 10^{12}	134

Rearranged product	k_r (s⁻¹)	P450 system	k_t (s⁻¹)	ref
Ph \ OH (allylic alcohol structure)	3.0×10^{11}	CYP2B1, Rat liver microsomes, CYP2B4	1.3×10^{12} 2×10^{9} to 1.5×10^{12}	134 135
Ph \ OH (allylic alcohol structure)	1.5×10^{11}	CYP2B1	4×10^{12}	135

Rearranged product	k_r (s^{-1})	P450 system	k_t (s^{-1})	ref
	1.5×10^{11}	CYP2B1	4×10^{12}	135

Rearranged product	k_r (s^{-1})	P450 system	k_t (s^{-1})	ref
Ph, OH	1.2×10^{11}	CYP2B1	$>1.2 \times 10^{13}$	135
$p\text{-C}_6\text{H}_4\text{CF}_3$, OH	9×10^{11}	CYP2B1	4×10^{12}	135

Rearranged product	k_r (s^{-1})	P450 system	k_t (s^{-1})	ref
p-C$_6$H$_4$Cl, OH	4×10^{11}	CYP2B1	5×10^{12}	135
OH	3×10^{11}	Rat liver microsomes, CYP2B1	1.4×10^{13}	136

Rearranged product		k_r (s^{-1})	P450 system	k_t (s^{-1})	ref
		4.4×10^7	CYP101, CYP102, CYP1A2 CYP2C9, CYP2C19, CYP2D6, CYP2E1, CYP3A4	$0.7 - 12.5 \times 10^{10}$	129,130
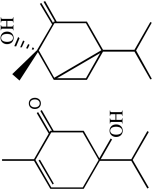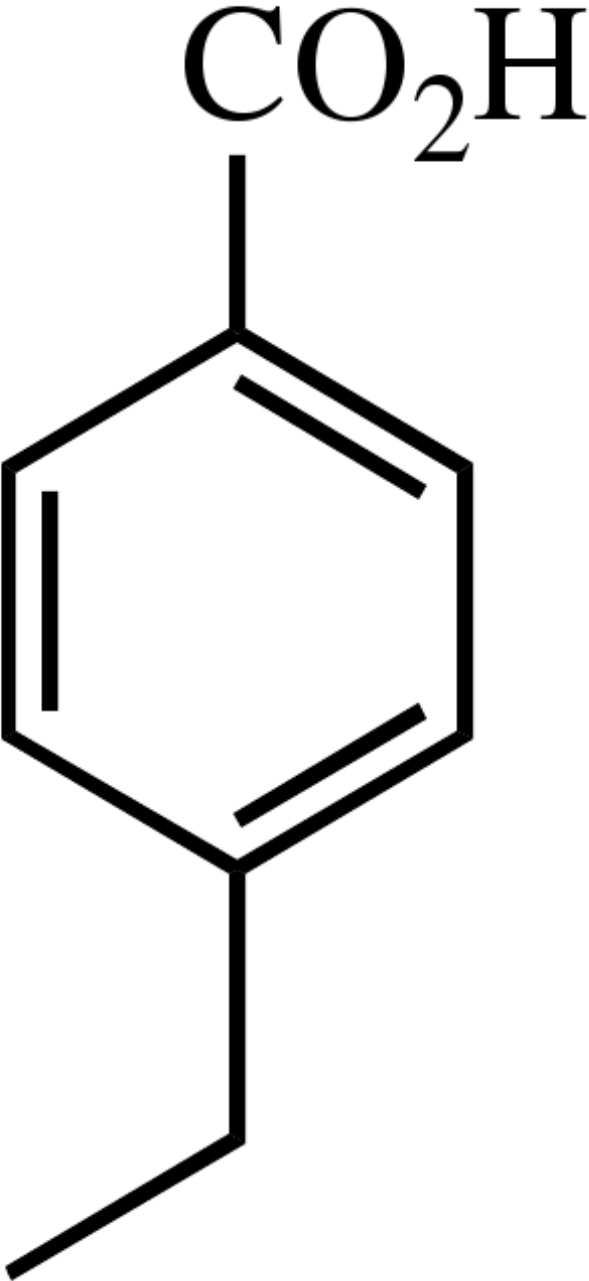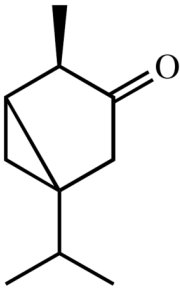
Rearranged product	k_r (s^{-1})	P450 system	k_t (s^{-1})	ref

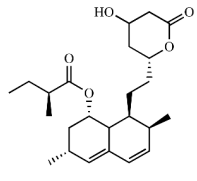| Rearranged product	k_r (s⁻¹)	P450 system	k_t (s⁻¹)	ref
	1.0×10^8	CYP101, CYP102, CYP1A2 CYP2C9, CYP2C19, CYP2D6, CYP2E1, CYP3A4	$0.7 - 12.5 \times 10^{10}$	129,130

Table 2

Examples of substrates that are oxidized by cytochrome P450 enzymes at a given carbon to both the hydroxylated metabolite and a desaturated product.

	Substrate	
21	CO_2H	

Substrate	
22	

Substrate
23

	Substrate	
24		
25		
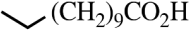
	Substrate	
26	$\diagdown$(CH$_2$)$_9$CO$_2$H	

Table 3

Bond strengths of selected C-H bonds

Bond	kcal/mol	Reference	Bond	kcal/mol	Reference
CH_3-H	104.9	155,156	$C_6H_5CH_2$-H	89.7	155
CH_3CH_2-H	101.1	155	$(CH_2=CH)_2CH$-H	76.4	156
Me_2CH-H	98.6	155	CH_3OCH_2-H	95.7	157
Me_3C-H	96.5	155	H_2NCH_2-H	92.2	158
$CH_2=CH_2CH_2$-H	88.8	155	$CH_2=CH$-H	108.9	159